UNIVERSIDADE D
COIMBRA

HAFIZA AYESHA KHALID

INFLUENCE OF N ADDITIONS ON THE STRUCTURE, MORPHOLOGY, THERMAL STABILITY AND TRIBOLOGICAL PROPERTIES OF W-S-N COATINGS DEPOSITED BY SPUTTERING

VOLUME 1

Dissertation under the Joint European Master's Degree in Surface Tribology and Interfaces guided by Dr Filipe Fernandes and Dr Talha Bin Yaqub presented to the Department of Mechanical Engineering of the Faculty of Science and Technology of the University of Coimbra.

July 2021

1 2 9 0

FACULDADE DE CIÊNCIAS E TECNOLOGIA
UNIVERSIDADE D COIMBRA

Influence of N additions on the structure, morphology, thermal stability and tribological properties of W-S-N coatings deposited by sputtering.

Submitted in Partial Fulfilment of the Requirements for the Degree of European Joint European Master in Tribology of Surfaces and Interfaces.

Influência da adição de N na estrutura, morfologia, estabilidade térmica e resistência ao desgaste de revestimentos do sistema WSN depositados por pulverização catódica

Author

Hafiza Ayesha Khalid

Advisor[s]

Dr. Filipe Fernandes

Dr. Talha Bin Yaqub

Jury

President	**Professor Doutor Bruno Trindade** **Professor at University of Coimbra**
Vowel	**Professor Doutor João Oliveira** **Professor at University of Coimbra**
Advisor	**Doutor Talha Bin Yaqub** **Researcher at Instituto Pedro Nunes**

· U C ·

UNIVERSIDADE DE COIMBRA

tribos Joint European Master in Tribology of Surfaces and Interfaces

Ljubljana • Leeds • Coimbra • Luleå

Coimbra, July 2021

ACKNOWLEDGEMENTS

I would like to express my gratitude to all who have contributed to completing the project described in this thesis.

First and foremost, I would like to thank my advisors, Dr Filipe Fernandes and Dr Talha Bin Yaqub from the University of Coimbra, for their guidance and valuable input during the project. I am gratefully indebted to Dr Manuel Evaristo and Dr Todor Vuchkov, who helped in the hardness and tribological characterization. Also, to Carlos Patacas of IPN for all the technical contributions for this work.

Special thanks to the TRIBOS consortium for providing me with this life-changing opportunity and the European Commission's funding. I wish well for my TRIBOS mentors Professor Ardian Morina, Professor Mitjan Kalin and Professor Bruno Trindade for, their support.

Finally, I want to express my profound gratitude to my parents, family, and friends who have offered constant support and encouragement, directly or indirectly, throughout this degree and while writing this thesis.

Abstract

TMD coatings are a breakthrough in the aerospace and automobile sector where low friction and low wear is required, along with the coatings ability to withstand harsh and humid environments. The current study aims to systematically characterize the influence of N additions on structure, morphology, hardness, tribological behaviour and thermal stability of WSN coatings deposited by sputtering. By varying the N_2 flow into the deposition chamber, four coatings with N content ranging from 0 – 21.9 at. % were deposited. The highest S/W ratio of 1.5 was exhibited by reference WSN0 coating. Total film thicknesses and the Cr interlayer and gradient layer were in the range of 2.1 – 2.4 µm. Reference WS_2 coating had a crystalline structure, whereas with increasing N at. % content coatings exhibited broad XRD diffraction peaks as a result of the contribution of two different phases. Coating with the highest N concentration displayed an amorphous structure. Coatings were characterized tribologically against 100Cr6 steel ball in SRV tribometer at room temperature and 200°C. Wear rate analysis showed that W-S-N coatings tested tribologically at high temperatures performed better than the coatings tested at room temperature. Thermal stability was determined by annealing the coatings at 200°C and 400 °C. No visible changes in the morphology and structure of the coatings were noticed with heat treatment. However, hardness behaviour showed a positive increase in the values after annealing at 400 °C.

Keywords: TMDs, WSN films, structure, high temperature tribology, annealing

Resumo

A aplicação de revestimentos do tipo TMDs no setor aeroespacial e automóvel têm permitido avanços significativos em componentes onde baixo atrito e baixo desgaste são necessários, juntamente com a capacidade dos revestimentos de resistir a ambientes hostis e húmidos. O presente estudo visa caracterizar sistematicamente a influência da adição de N na estrutura, morfologia, dureza, resistência ao desgaste e estabilidade térmica de revestimentos do sistema WSN depositados por pulverização catódica. Variando o fluxo de N2 na câmara de deposição, 4 revestimentos com teor de N (entre 0 e 21,9 at. %) foram depositados. O revestimento de referência A razão S/ W mais alta de WSN0 apresentou a razão mais alta de S/W. A espessura total dos filmes juntamente com a intercamada de Cr e a camada de gradiente encontra-se entre 2.1 – 2.4 µm. O revestimento de referência apresenta uma estrutura cristalina. O aumento do teor de N nos revestimentos resulta num alargamento dos picos de difração devido à contribuição de duas novas fases. O revestimento com maior concentração de N apresenta uma estrutura amorfa. Os revestimentos foram caracterizados tribologicamente num equipamento SRV contra uma bola de aço 100Cr6 à temperatura ambiente e a 200 °C. Os revestimentos W-S-N testados tribologicamente aalta temperatura apresentaram um melhor desempenho que os revestimentos testados à temperatura ambiente. A estabilidade térmica dos revestimentos foi avaliada a 2 temperaturas distintas (200 °C and 400 ^{0}C), onde não se observaram alterações estruturais e morfológicas.

Palavras-chave: TMDs, Revestimentos do Sistema WSN, Estrutura, Tribologia a quente, Recozimento

[LIST OF FIGURES]

[LIST OF TABLES]

[LIST OF SIMBOLS] AND [ACRONYMS/ ABBREVIATIONS

[List of Symbols]

℃ – Degrees Celcius

k – Specific wear rate

E – Módulo de Elasticidade

H – Hydrogen

C – Carbon

N – Nitrogen

Ar - Argon

[Acronyms/Abbreviations]

TMD – Transition metal dichalcogenide

PVD – Physical vapour deposition

MoS_2 – Molybdenum disulphide

WS_2 – Tungsten disulphide

NASA – The national aeronautics and space administration

TMD-C – Carbon doped transition metal dichalcogenide

DLC – Diamond like carbon coatings

CH_2 and C_2H_4 – Methane and Ethylene

H_2 – Hydrogen gas

H_2S – Hydrogen sulphide gas

N_2 – Nitrogen gas

DCMS – Direct current magnetron sputtering

CO_2 – Carbon dioxide

CVD – Chemical vapour deposition

TiC – Titanium carbide

CrN – Chromium nitride

WC – Tungsten carbide

TiAlN – Titanium aluminum nitride

TMD-N – Nitrogen doped transition metal dichalcogenide

FCTUC – Faculdade de Ciências e Tecnologia da Universidade de Coimbra

DEM – Departamento de Engenharia Mecânica

CONTENTS

CHAPTER 1

1. INTRODUCTION

Today's society is dependent on transportation, manufacturing, and power generation industries. Since the inception of mobility by humans, there have been various types of material studies, development of different machines and their components, productions being executed by various equipment consisting of several mechanical components that require surface interactions. These surface interactions are mainly governed by a field of science known as tribology. Tribology is the field of science that deals with the interaction of surfaces in relative motion. Some of the applications where tribology is involved include car engines, piston rings, bike chains, air foil bearings, journal bearings, mechanical gas seals, rolling element bearings, gears, viscous dampers, fluid film bearings, magnetic storage devices, power plants and bio-medical implants [1], [2].

TMD compounds are under research for decades as potential solid lubricants. Previously, TMDs were used as additives in oil lubricants, particularly MoS_2, since NASA used them early ’60s [3]. Nowadays, they are being used as solid lubricants deposited mainly by physical vapour deposition (PVD) as thin films with a major focus on WS_2 coatings [4]. Other TMDs, i.e., diselenides and tellurides of molybdenum and tungsten, are not much studied despite having similar layered lattice structures, possibly due to much higher cost [4], [3].

The sliding efficiency of TMDs could only be improved by developing this coating system with good mechanical strength, high hardness, improved adhesion, high density, and low porosity with optimum stoichiometry. Thus, TMDs have been alloyed with different metals, non-metals, and compounds [4].

Due to cost-cutting and simpler processes, non-metal doping is preferred in most industries over metal doping. Among non-metal doped TMDs, carbon addition has shown significant improvements in tribological performance with almost one order of magnitude improvements in hardness. Previously, TMD-C thin coatings were prepared in the presence of CH_4 gas. These thin films exhibited improved hardness, density, wear resistance and low co-efficient of friction with varying the carbon content by changing the gas flow inside the chamber. The principal aim was to combine the lubricious effect of TMDs in a vacuum and

the good mechanical properties of DLC coatings in a humid environment. However, enhancement in properties was achieved at the expense of stoichiometry and crystallinity.

Similarly, TMD-C systems testified to have fluctuating friction coefficient and wear rate in diverse environments. Likewise, the literature sometimes contradicts properties improving in one case while showing an inverse trend in other cases. Consequently, despite their stable conduct in dry and humid environments, their tribological efficiency still needs improvements [5]. Like tribo performance, the mechanical properties, especially hardness, also needs further enhancement. Hence, a stable coating with consistent tribological and mechanical properties in diverse environments would be taken as a quantum leap. Having said this, it is no surprise that there is still room for improvement in these coating systems.

To fix the problems of existing solid lubricious green coating systems, TMD-N seems to be a promising solution unveiling low friction and wear rates and improving mechanical properties and oxidation resistance. However, this area has not been explored enough in comparison with the TMD-C system. N_2 doping offers several advantages such as i) gradient layer of metal nitride can be easily developed for coating adhesion improvements, ii) in case of C alloying, the sputtering chamber needs a carrier gas, e.g., CH_4 and C_2H_2 which leads to impurities in the system and disturbs the stoichiometry (low chalcogen atom to metal ratio) due to the combination of H_2 with chalcogen atom, e.g., H_2S while N_2 alloying is carried out by reactive sputtering, so, as a precursor pure N_2 gas is used which can potentially minimize the impurities in the system, iii) absent impurities, N_2 alloying might also lead to a stable coating with no potential worn material, as N can escape as N_2 gas from the contact zone, iv) industrial depositions need cost-effectiveness of the deposition setup. TMD-N coatings depositions need only N_2 precursor gas, so it is more cost-effective than TMD-C deposition, where an additional C target is needed if we want to replace reactive sputtering and the adverse effects of the precursor gasses, v) incorporating N may improve mechanical properties, thermal stability, and oxidation resistance of the coatings.

Thesis aim

The proposed thesis aims to contribute to developing transition metal di- nitrides/sulfides $TM(S, N)_2$ films deposited by direct current magnetron sputtering with varying N content.

Significantly harder, more oxidation resistant and low friction properties are the goals for the coatings to be developed. The practical aim is to increase the hardness of coatings through nitrogen additions and systematic study of its influence on the morphology, structure, mechanical and tribological properties. Moreover, as literature lacks reports on the effects of heat treatment (annealing) on the compositional, morphological structural, and mechanical properties of these coatings, this will also be one of the potential domains explored during this research work.

To accomplish the main objective of this thesis, the following sub-objectives should be achieved:

1. Deposition of W-S-N coatings (with increasing N concentration) using DC reactive magnetron sputtering and their comparison to pure WS_2 coating. Optimization of the interlayer to ensure the good adhesion of the films to the substrate.
2. Characterization of the morphology, structure, mechanical properties, and adhesion of the coatings.
3. Evaluation of the thermal stability of the developed coatings under protective atmosphere. This will be followed by the comparison of these coating with non-annealed ones.
4. Investigation of the influence of N additions on the tribological performance of coatings at room and high temperature (200 ^{0}C). Study of the wear mechanisms and their correlation with the friction coefficient and specific wear rate values.

Thesis organization

This thesis draft is composed of 6 units. ***Chapter 1*** introduces the needs for advanced lubrication techniques with an overview of TMDs with the objective of this research. ***Chapter 2*** deals with the economic importance of proper lubrication and evolution of solid lubricant coatings from graphite to TMDs, issues of pure TMDs, their mitigation with C and N-alloyed TMDs and the advantage of N-alloyed over C-alloyed solid lubricant coatings. Lastly, the development of W-S-N coatings over the years till date, the research gaps and the aim and objectives of this research work. ***Chapter 3*** covers the materials used for substrate, deposition technique and characterization techniques followed. ***Chapter 4*** presents and discusses the results in detail along with literature comparison. In ***Chapter 5***

the crux of this research is concluded with the future work in ***Chapter 6***, respectively to be done to carry out this work.

CHAPTER 2

2. STATE OF THE ART

Whenever tribo-interactions are involved in any system, they are quantified through friction, wear, and lubrication. Controlling friction and wear through proper lubrication are the preliminaries for an efficient long-lasting performance of components / parts in any industry [6].

2.1. Liquid lubricants, problems, and remedy

One of the most common and traditional ways of reducing friction in any mechanical system is liquid lubricants. By volume, the minerals oils constitute the largest portion of lubricants that are used worldwide. Lately, they are being replaced by synthetic oils due to their poor thermal and oxidation stability. Also, the shelf life of the latter is comparatively high. Liquid lubricants provide good wetting and adhesion during shearing mechanisms. Their load carrying capacity and viscosity index have been improved over time by adding additives like viscosity modifiers, anti-friction, and anti-wear additives [7]. With nanotechnology-based friction modifiers and anti-wear additives, the structural properties of liquid lubricants can be tailored. This can help to attain a friction coefficient as low as 0.005, even in boundary lubrication regime, despite very thin film thickness. Universally, carbon-based additives containing nano-diamonds, domain-like carbons, carbon nanotubes, graphene and graphite are widely used. Due to the toxic nature of organic additives, they are being replaced with some inorganic fullerenes of transition metal dichalcogenides (TMDs), copper, polymeric and boron-based nanoparticles [8]. Among liquid lubrication, to minimize the inactive lubricant volume and viscous losses, vapor phase lubrication is another method for systems where lubricant is needed only in a small portion, for instance, in roller bearings. This method is also helpful in high temperature operating environments where ordinary lubricants lose their efficiency, and the capillary action of lubricants is problematic such as in microelectromechanical systems (MEMS) [9], [10].

Despite fruitful results, liquid lubrication has some major drawbacks and limitations. Such systems need high maintenance and their use in extended environments for longer periods have posed limitations due to issues like low oxidation stability, frequent viscosity changes, high thermal degradation, low volatility, high toxicity, and high flammability etc. It is impossible to change lubricants after all certain miles or hours in a running system, which might result in efficiency loss. It is obvious that liquid lubrication is neither possible nor recommended in extreme environment high tech systems or situations where liquid can become a contamination source in the system e.g., optical systems and food industries. Other major issues with liquid lubrication today are related to the depleting fuels resources, escalating industrial demands, challenges for CO_2 emissions which might hinder the development of a sustainable society [6].

To mitigate these drawbacks, self-lubricating coatings were introduced as a medium of surface treatment for resistance to wear and friction during a tribo contact. The advantages of solid lubricant coatings include: (i) ease of usage and handling, (ii) high wear resistance (iii) low cost of production and maintenance and (iv) lightweight materials. All these benefits are obtained without compromising the mechanical strength and base material designs [11]. Consequently, the design and development of solid self-lubricating coatings became an attractive subject of fundamental and applied research.

2.2. Solid lubricants

Recent scientific developments have introduced solid materials which can be used as lubricants to reduce wear and friction between sliding contacts when loaded in service conditions, such as liquid lubricant additives, free flowing powders, grease additive, anti-freeze paste and anti-friction coatings. The mechanism in suppressing the contact stresses and facilitating motion involves the adherence of solid lubricant to the substrate and level the asperities by filling in the valleys of surface roughness [16]. Regardless of the load, speed and temperature, solid lubricants maintain an unvarying film thickness and bear load with easy shearing ability. These characteristics of solid lubricants permits effective replacement of liquid lubricants [11]. Surface engineering revolutionized the world of solid lubrication with the introduction of the thin solid coating's domain. Thus, in present era, solid lubricants are mostly applied as thin coatings.

2.3. Classification of solid lubricants

So far solid lubricant coatings can be classified into four groups: single component coatings, multi-component coatings, gradient or nanostructured coatings and smart coatings. *Single component* coatings have one or two components and are produced by low-cost deposition techniques like CVD and PVD. Some examples are TiC, TiN, DLC, WS_2, MoS_2, CrC, CrN, WC/C and soft metals due to their numerous shear planes. Their limitations regarding friction coefficient, wear rates and thermal stabilities led to the development of multicomponent coatings [11]. A periodic repetition of phases or components (particles and fibers) of a single component coating forms a *multicomponent coating* of few microns, where each sub-film is in um range. This composite nature results in diffusion barrier and low friction, while at the same time impedes dislocation movements to improve the mechanical properties of the coating [17]. *Gradient coatings* e.g., TiAlN (hard phase) + MoS_2 (soft phase) consist of nanostructured grains of softer material embedded in an amorphous matrix, providing high adhesion, toughness, and hardness along with low friction and wear at nanoscale while low elastic modulus at macroscale. Gradient layers also mitigate the drastic hardness transition from coating to the substrate, which is very crucial for a sustainable and efficient tribo coating [18].

Solid lubricants which retain their properties with environmental shifts are called smart, self-adaptive or *chameleon coatings*. Usually, these coatings are doped/alloyed with metallic or non-metallic elements to develop an efficient sliding system for diverse environments. One example is the WC/DLC/WS_2 coatings, where WS_2 and WC nanograins are embedded in a:C matrix. These coatings can show self-adaptive behavior with WS_2 playing the dominant role in vacuum or dry environments, while C is responsible for low friction in humid atmosphere. When exposed to high temperatures WS_2 crystallized and re-oriented and carbon was ejected out in form of graphite from a:C matrix, providing self-adaptive behavior. Desired behavior of DLCs in humid environment is combined with behavior of WS_2 in vacuum, making smart coatings a breakthrough in the tribology industry [19].

2.3.1. Lamellar solid lubricants

Two most widely used solid lubricants with lamellar structure are carbon-based materials and TMDs. In this chapter carbon-based materials will be discussed briefly followed by comprehensive discussion on TMDs in accordance with the thesis objective.

2.3.1.1. Carbon based materials

Graphite is the most used carbon-based lubricant. It owes its lubricity to the lamellar crystal structure where weak Vander Waal's forces facilitate the easy shearing of the basal planes and reduce friction. However, the slippage of basal planes exposes the dangling bonds to other edge sites, damaging the basal planes and thus increases adhesion gradually [20]. Later, the researchers discovered that shearing is favored by humidity since moisture passivates these free dangling bonds to minimize surface free energy along with protection from bonding with other edge sites [21].

Another carbon bases solid lubricant coatings are the DLCs which showed high hardness, high young's modulus, low friction, and wear characteristics which made them stand out as lubricious coatings, however, they cannot be classified under lamellar coatings. In the DLC coating, Sp^3 hybridization results into diamond like structure which gives very high hardness, chemical stability and wear resistance, whereas Sp^2 hybridization is a dominant characteristic of graphite and due to weak Van der Waals interactions, it behaves as a lubricant [22]. However, as a remedy to poor adhesion resulting from low toughness and residual stresses doping with metals and non-metals was introduced and enhanced the tribological properties. Moreover, just like graphite, the properties of DLCs degrade in the absence of moisture. To overcome this issue and to enhance their performance in dry and vacuum environments, hydrogenated DLCs were introduced. But unfortunately, hydrogen was affecting the performance of these coatings in humid conditions, so, it was reported that hydrogenated DLCs performed better in inert and dry conditions while hydrogen free DLCs showed low COF ~0.1-0.15 in humid environments [23].

Overall, DLCs provide high hardness, friction coefficients in the range of 0.09-0.3 and good wear resistance under certain dry conditions. DLCs, however, have few drawbacks: i) if there are residual stresses in the films, they tend to gradually increase the wear rates due

to their flaking from the substrate, ii) they fail to provide efficient lubrication in vacuum environments due to the lack of the dangling bond passivation, iii) hydrogenated-DLCs although provide satisfactory results in vacuum, they are not so much suitable for humid air sliding and finally, iv) their potential use is limited in application demanding high temperature operative environments due to a relatively low thermal stability (< 400°C). Likewise, the ineffective lubrication of polymers and soft metals attributed to their thermal instability and poor heat transfer capacity, restrict their use as solid lubricants [12].

2.3.1.1. Transition Metal Dichalcogenides

TMDs are compounds of transition-metal atoms (group vi: Cr, Mo, W, Nb) and chalcogens atoms (group x: S, Se, Te) - have appealing lubrication properties. The lamellar structure of transition metal dichalcogenides, MX_2 (where M is Mo, W, Nb, Ta, etc., and X is S, Se or Te) are no less than a gift of nature, since these materials can provide very low frictional properties and if properly optimized, they are very well suited for various tribological applications. TMDs consists of a layered crystal structure in which the chemical bond within the atomic layer (metal and dichalcogenide atoms) is strong covalent bond, however, weak Van der Waals interactions exist between adjacent lattice layers. As a result, preferential sliding occurs between the weekly bonded lamellae, providing low friction [24], [25]. TMDs exist in two crystal forms: hexagonal and rhombohedral [4]. In accord with the thesis aim, only hexagonal structure with six-fold-symmetry (two molecules per unit cell) will be discussed. This is the structure giving lowest friction properties due to occupied outer d-orbital. The anisotropic attributes of TMDs originated from their exclusive strong covalent intralayer bonding and weak Vander Waal's interlayer bonding cause them to have easy slide under rubbing conditions.

Applications

Due to the direct band gap in TMD monolayer, it can be used in electronics as transistors and in optics as field effect emitters and detectors. Their prospective use as a replacement of silicon in advanced electronic devices or ultimately, the whole electronic circuit made with TMDs put emphasis on their detailed study [26]. On the other hand, TMDs are potential replacements of liquid and other solid lubricant in aerospace industry for terrestrial and non-terrestrial environments. Recently, fullerene like TMDs and TMD

nanotubes as additives in liquid lubricants and thin coatings are the limelight of solid lubricant exploration [4]. MoS_2 and WS_2 are widely used TMDs among the lowest friction coatings where MoS_2 is accessible from nature as molybdenite while WS_2 and other TMDs like WS_2, $MoTe_2$, $MoSe_2$, and WSe_2 are synthesized [27].

2.3.1.1. Factors affecting the performance of TMD films.

The friction coefficient of these dichalcogenide coatings is highly dependent on in-service conditions, temperature, load, speed as well as other factors like film thickness, stoichiometry, crystallinity, and purity etc. Apart from low friction properties of TMDs in dry atmosphere or vacuum, humidity is known to have detrimental effect on their lubricity and lifespan with typical values of friction coefficient increasing up to 0.01 - 0.25. At higher temperatures TMDs have a very high probability of oxidizing which causes the thermal degradation of coating [28]. Although, the initial use of TMDs reports back to the coatings developed by burnishing, the thin sputtered films have better lifespan and lower coefficient of friction than the former. In advanced physical vapor deposition methods, sputtering is the widely used approach to produce thin TMD films such as magnetron sputtering, in comparison with ion beam assisted deposition and ion beam mixing, has reported to produce films with better tribological properties [29]. The pure sputtered TMDs are highly porous and columnar. Studies have shown that coatings with porous columnar structure leads to low load bearing capacity, film deterioration and removal from tribo-contact even though the friction coefficient is low. During sliding, the columns of coatings break tear off and during this, the randomly oriented TMD crystals reorient such that the basal hexagonal plane (002) aligns parallel to the sliding surface resulting in easy slide of two surfaces. Sometimes these flakes are detached from the contact but are immediately restocked from underlying surface through the same reorientation process. The reorientation is dependent on the as deposited microstructure and % of crystallinity of the coating. Overall, the pure MoS_2 coatings free of oxygen has revealed the lowest coefficient of friction with values 0.002 – 0.01 [30], [31]. Along with the morphology and microstructure, the stoichiometric changes greatly influence the tribological performance due to the existence of foreign entities either in form of contaminants that may come from deposition chamber (e.g., O/C/H or dopant materials added to enhance the compactness, adhesion and suppress the wear rate and coefficient of friction. Nevertheless, pure TMD coatings have

the lowest coefficient of friction, but their use is restricted due to poor adhesion and accelerated wear rate. Similarly, crystal defects can lead to poor performance, however, sometimes it is beneficial in case of superlattice effect. TMD coatings deposited with sputtering without any contaminant and assisted orientation of basal plane in ultra-high vacuum outperform the other coatings in terms of low coefficient of friction [32].

2.3.1.1. Comparison between TMDs and DLCs

Despite the frequent use of DLCs as low friction and low wear coatings, unlike TMDs due to the presence of hard amorphous carbon, DLCs are not classified among the tribo-active coatings – coatings that actively tries to facilitate the tribological properties. DLCs are made tribo-active with the help of outside atmosphere and oil additives, these additions in comparison with DLCs may negate the beneficial properties of TMDs. On the other hand, the tribolayer in TMDs is already passivated unlike DLCs and the mutual repulsion between the layers due to similar (positive) charge results in easy shear of basal planes [33]. Another major issue of DLCs is the graphitization resulting in high sp^2 content at very high temperature, hence, causing a rampant increase in the friction and wear leading to coating failure. DLCs are not recommended to be used in vacuum environments and with the combination of carbon with air it produces CO_2 thus restricting them for long-term applicability in dry/vacuum atmosphere and at elevated temperatures higher than 300^{o}C. Contrarily, TMDs exhibit low friction and wear even at elevated temperatures due to the removal of absorbed water but the issues of high temperature oxidation may come into play [34]. In next section more details about TMDs, drawbacks of pure TMDs, alloying of TMDs, and especially, N alloying is reported.

2.4. Tribology of transition metal dichalcogenides - A walk through

The lowest possible shear of TMDs is acquired through a particular electronic structure having outer d-orbital filled together with hexagonal lamellar crystallographic structure. These fundamental requirements restrict TMDs to a smaller group of compounds (MoS_2, WS_2, $MoSe_2$, $MoTe_2$, WSe_2, etc.) that potentially come under the spectrum of low friction

coatings. The shear-ability of MeX_2 originates from its anisotropic nature having transitions metal layer packed in between the chalcogen atom layers [4].

The unsaturated and dangling bonds are present on the edges of the planes due to their lamellar structure. These dangling bonds are susceptible to oxidations. Therefore, the electrons are favorably clustered near metal layer leaving a net positive charge on the surface of sandwich, causing repulsion between two adjacent sandwiched layers. Attributable to this unique layering arrangement, low friction properties are achieved in TMDs [21].

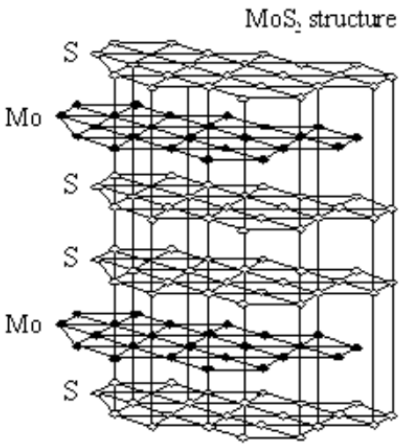

Figure 1: Layered structure of MoS_2 solid lubricant

2.4.1. Tribofilm formation

Tribofilm formation is the key process for low friction properties in vacuum and dry contact where, during sliding under load, the basal planes reorient themselves in the direction of motion to form tribofilms. These tribofilms are very soft and easily shearable, thus providing low friction. As deposited coatings have reported to have planes in an unsought orientation. Application of load causes the newly formed tribofilm to reorient the (002) shearing plane along the sliding direction. While running in period, some of tribofilm may dispense along with impurities from the contact proving beneficial for the system. In the beginning the coefficient of friction and wear is high as asperities are being deformed but once a uniform tribofilm is formed the system becomes independent of the need of repeated lubrication as in fluid-based systems [21]. Primarily, the coating is worn and sheared due to mutual repulsion between TMD layers. Later, after some initial wear, the coating from underneath transforms to replenish the TMD tribofilm by reorientations under sliding contact. The friction coefficient is dependent on the transfer of coating to the counter body and reorientation However, everyday conditions are not perfect and humidity influence from atmosphere depreciates the low friction and wear attributes of TMDs. Strong hydrogen bonds are formed due to the attack of water molecules at defects and edges due to the presence of unsaturated bonds and sometimes combination of water with sulfur and selenium. Hence, chemical, and electronic structure is altered in such a way

that mutual repulsion between TMD layers changes to mutual attraction and reduces shearing [35], [34].

Anyway, the time required for tribofilm formation is called running-in time. This time is affected by coating characteristics such as composition, stoichiometry, hardness, roughness, and operating environment such as sliding speed, number of laps, moisture, load, and temperature. Once the tribofilm is formed, the arrangement behaves like fluid system. At this stage, it is impossible to differentiate the planes along which easy shearing is taking place. The sliding takes place solely inside the tribofilm through shearing over the low shear strength basal planes. Due to these formations of tribofilm, TMDs appear to be a superior substitute for liquid lubricants as they will also help to overcome issues like cold start and fluid volatility [2].

2.4.2. Problems of pure TMD coatings

Cavaleiro et al. [4]*,* [2] reported the possible limiting factors for the restricted use of pure TMDs. They concluded that:

1. Pure TMD films are porous and has columnar morphology which makes it easier for oxygen, water, and other reactive species to penetrate the film and reduce low frictional characteristics. Disulfides are more sensitive to water than diselenides. High porosity and columnar morphology reduce the adhesion to substrate, mechanical properties, and load bearing capabilities of the coatings. Pure TMDs have very low hardness of only 0.3-2 GPa. It is easy for coating of this hardness to be chipped off during sliding under high pressure exposing the substrate to environment, thus resulting in very high wear rate.

2. The presence of lamellar planes in TMDs also causes exfoliation/delamination at low loads. This results in providing lower scratch resistance due to poor mechanical cohesion. Also, due to the lack of adhesion with substrate, the coatings tend to flake off entirely which results in higher wear and friction.

3. Magnetron sputtering produces a disordered structure where (002) planes which are mainly responsible for superlubricity are almost always randomly oriented.

While, to achieve low friction, these planes should have a preferential orientation parallel to the coating surface.

4. Their extreme sensitivity to environmental attacks like oxygen and moisture while sliding in humid air and high temperatures, respectively is very likely due to the reaction of dangling bonds with these elements. Only well oriented basal plane parallel to surface will be immune to such reactions. Another disadvantage they offer is difficulty in storage of these films because they deteriorate with time because of environmental attacks.

2.4.4. Alloying of TMD coatings

As a remedy to aforementioned problems, TMDs are strengthened structurally and chemically by the addition of impurity atom in the lattice structure just like alloys. For this purpose, MoS_2 and WS_2 were doped with metals, for instance, Ti, Al, Au, Pb, Ni, Cr and Fe. Iron was the first element with which MoS_2 coatings were doped in 1970s and resulted in a composite coating with compound $FeMo_4S_5$. After 2 hours of testing, friction coefficient was reported to be 0.18. Ti doped films exhibited lower COF and wear rate, also provided protection against oxidation. Nonetheless, Ti doped coatings also failed during testing at high temperatures. Even though load bearing capacity, adhesion, and density of Ti doped TMDs were superior to pure TMD films but delamination still persisted since flaking off of crystalline interfaces accelerates the wear rates. Later, other metal alloying dopants were explored but due to the depletion of metal dopant with time through diffusion and high costs due to low deposition rate and usage of multiple targets, metal doping is not considered viable industrial implementation [4]. Moreover, metal dopants provide hinderance to efficient tribofilm formation and their low temperature thermal stability results in oxidation of some metals such as Ti ensuing wear abrasive particles in the tribo-system. Additionally, literature suggests a very low metal dopant percentage which leads to porous and columnar structure of the coating impacting the tribological performance and load bearing capacity. Also, literature provide insufficient data on the performance of metal doped coatings in ambient, vacuum, dry and high temperature cyclic environments [4], [21], [26]. Most explored TMD films with non-metallic alloying are based on carbon alloying, which exhibited better mechanical and tribological performances compared to

pure TMD coatings. The combination of exceptional low frictional behavior of TMDs in vacuum and dry atmosphere with the mechanical strength of a:C resulted in an overall enhanced tribological properties for diverse environments. W-S-C system was first introduced by *Voevodin et al.* [5] in late 1990s where it was noticed in an amorphous dense carbon matrix, nano crystallites of WS and WC phase are uniformly dispersed. He reported to have observed the chameleon behavior of the W-S-C coating during sliding in ambient air and vacuum environments. It was noted that with C alloying, nano-layered structure is difficult to deposit industrially with standard conditions. Moreover, to deposit TMD-C coatings, either an additional graphite target or the use of a precursor gas i.e., CH_4 is required. The impurities induced in coatings due to the presence of H and the reduced effectiveness of WS_2 targets in CH_4 containing environment deem fruitless, thus, leaving graphite targets mandatory in the deposition chamber [4], Also, the additional source of power is required while using graphite targets to obtain a freedom to play with the stochiometric balance, microstructure, and morphology of the composite coating [36]. The use of multiple targets, although mandatory but it is not cost effective from an industrial perspective and large-scale applicability of this coating system. It should also be pointed out here that despite the use of multiple deposition approaches (reactive sputtering, composite targets, multiple targets), the improvements in the morphological and mechanical properties were not up to expectations. This means that the achieved hardness was in the range of 4-10 GPa which is quite low when compared to DLCs and other solid lubricant coatings. Additionally, these improvements were achieved at the expense of low film stoichiometry and degradation of structural properties of TMDs in the C matrix. It is well known that the tribological properties depend on the degree of crystallinity and stoichiometry of TMDs as well as the mechanical properties, this system is not efficient enough as a sustainable tribological solution for low wear and friction. Moreover, considering the requirements of additional target, the cost of the process also becomes higher which is against the industrial requirements. Hence, a new approach for evolution of TMD system is required with spiking industrial need for an efficient coatings system which would sustain high temperature as well as maintain their integrity in dynamic and cyclic environments, providing good tribological properties.

As an escape from the above discussed issues/problems, N alloying was tried by various researchers. Next sub-section of this chapter deals with an overview of TMD-N coatings. Only the most promising works will be discussed.

2.4.4.1. Nitrogen alloyed TMDs

Previous researchers have observed a considerable increase in hardness, compactness, and densification of TMD coatings after N-alloying. Additionally, significant improvements in adhesion and low friction and wear properties have been reported. Since hardness can be affected by many factors such as decrease in grain size, dense microstructure (compactness) and precipitation of harder phases in the composite. Hence, nitrogen alloying is a suitable option for developing coating that will sustain the high loads and provide better tribological properties in fluctuating temperatures, humidity, and dry atmospheres. However, TMD-N system has not been explored widely like TMD-C system. Thus, the true potential of the nitrogen as an alloying addition remains to be identified. *Liu et al.* [37], studied the effect of N+ implantation on the tribological properties of sputtered MoS_2 coatings. They observed 50 % decrease in film thickness due to densification of columnar structures. Also, N alloying reported to have threefold increase in wear life under ambient air (60-70 % relative humidity) and in high vacuum of 5×10^{-3} Pa. Moreover, during sliding contact these films exhibited good lubricating properties due to the orientation of basal plane along the surface (test conditions: F = 5.6 N, speed = 1000 rev/min). However, COF rises from 0.07 to 0.13 in ambient air and 0.04 to 0.06 in vacuum.

Since, MoS_2 and WS_2 were the most explored among other TMDs therefore, the early emphasis has been only put on MoS_2. Later, WS_2 became the limelight for advances in low friction coatings, owing to their better performance and oxidation resistance at higher temperatures (operating temperature limits for MoS_2 is 300 ℃ while for WS_2 is 400 ℃). Hence, only W-S-N coatings evolution will be discussed, keeping in agreement with the thesis scope.

Even though the N-alloying of MoS_2 films began in early 90s, the very first W-S-N system was developed by *Cavaleiro et al.* [36]. They synthesized ternary W-Ni-C/N films to study the influence of C/N percentages on the coating properties with varying nickel content. They also addressed the relationship of alloying additions and coating properties. These

films were deposited by reactive sputtering with increasing partial pressure of reactive gases (i.e., CH_4 and N_2). The increase in partial pressure led to an enhanced incorporation of alloying addition on the coatings. This effect along with higher substrate bias resulted in the incorporation of alloying elements in the interstitial sites, thus, modifying the structure of the coatings. They also observed an increase in compactness, resulting increased hardness (25 to 55 GPa). The young´s modulus followed similar trends as hardness with comparative adhesion result between W-Ni-C and W-Ni-N films.

Later in 2003 *Nossa et al.* [38] developed W-S-N films with an introduction of Ti interlayer for adhesion improvements. It was reported that N-alloying and the Ti interlayer combined to improve the hardness of pure WS_2 coatings from 0.6 GPa to 6 GPa. For coatings alloyed with 20 % nitrogen show a rise in COF in a range of 0.1-0.2 as the formation of WS_2 as 3rd body was difficult. However, no spalling was observed. Also, the scratch resistance increased, with adhesion critical loads increasing from 5 N to 25 N. Consequently, an increase in wear resistance was observed. These combined effects accumulated in the form of satisfactory tribological performance. Later for same coatings, *Nossa et al.* [39] noticed that W-S-C films exhibit better tribological behavior than W-S-N ones. Co-efficient of friction for higher N content increases to 0.9 towards the end of test whereas, in case of low N content it remains 0.2. Films with high N contents lose the tribological behavior, however, at high applied loads, the COF decreased due to the formation of tribofilms and transfer films. *Nossa et al.* [40] also revealed that films with 15 % or higher nitrogen percentages are amorphous, and the results were backed by XRD analysis which justifies the increase in hardness due to formation of new intrinsically harder nanocrystalline phases. Also, adhesion improvement was linked to the TiN phase between interlayer and film as shown in the Fig. 2 [40].

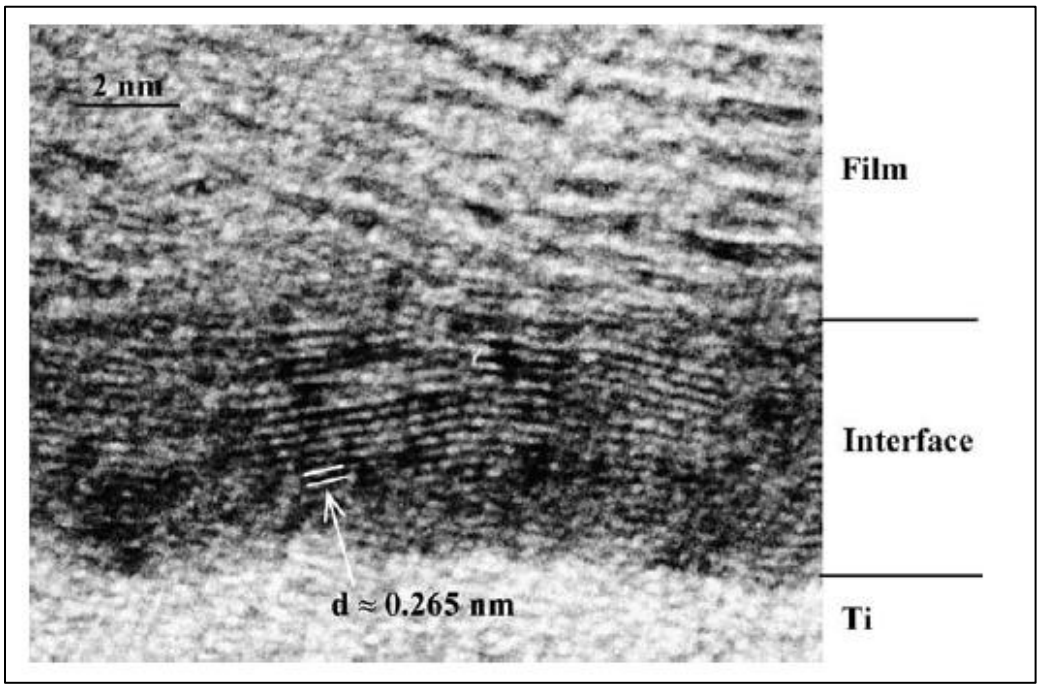

Figure 2: Cross-sectional TEM micrograph from the interface between the film and Ti interlayer

It was further observed that with the addition of N in the system, the coating display compact morphology and become deficient in sulfur. After pin on disk analysis of this film, the friction coefficient of less than 0.1 was achieved, which is better than pure WS films. However, the ball on disk test of pure WS_2 films revealed better wear coefficient due to their higher S content or in other words higher S/W ratio. Higher ratio allows easy and fast tribolayer formation, but the long-term durability of the system is still a question mark. The friction co-efficient for N doped films was in the range of 0.08 – 0.32 [41].

Gustavsson et al. [42] synthesized amorphous W-S-N coatings having featureless morphology. Ti interlayer was deposited before final coatings for adhesion improvements. A COF of 0.003 is reported for dry environment sliding for coating having 34 % nitrogen, 29 % tungsten, 25 % sulfur and 12 % oxygen. The reason for this extremely low friction coefficient was the formation of tribofilm at the contact interface and transfer film on the counter body. The underlying hard W-S-N matrix (below the tribofilm) provided support for basal plane orientation of tribofilm. This self-adaptability of coating characteristic also explains the damage recovery of coating despite being chipped off from some areas. Hence, amorphous W-S-N coatings appeared to be a promising candidate for ultralow friction.

Following this work, *Sundberg et al.* [43] studied the effects of composition, morphology, and testing environment on tribological performance of W-S-N films. Increase in friction and wear was observed in order of dry N_2 < dry air < humid N_2 < humid air. Also, high nitrogen content led to deficiency of sulfur and tungsten which could also account for wear and friction increase. It was suggested that to obtain reduced friction and wear, a continuous presence of WS_2 tribofilm is necessary with underlying amorphous W-S-N matrix. W-S-N films exhibited excellent tribological behavior in inert atmospheres (dry N_2) with COF ~ 0.02 and wear rates less than 100 $\mu m^3/Nm$. It was then concluded that moderate addition of nitrogen to WS_2 films can possibly make coatings not only mechanically strong but also result in ultralow friction.

Recently, an interesting work was published by *Isaeva et al.* [44]. in which the reason for ultralow friction of amorphous W-S-N coatings was reported. The study reports that 21 – 24% of N atoms form semi-free N_2 molecules located in the cages of W-S-N amorphous matrix. Coordination of these quasi-free N_2 molecules with atomic sulfur facilitate the W and S for easy WS_2 formation. It was concluded that ultra-low friction of W-S-N coatings originate from easy access of W and S for WS_2 formation, possessing dense and stable morphology leading to low friction and wear. Overall, this happens due to the release of nitrogen in N_2 gaseous form during sliding conditions.

In another study of W-S-N coatings, *Mutafov et al.* [45] further explored the structure, mechanical and tribological properties of N alloyed WS_2 coatings with a dominant (002) orientation were deposited by DC reactive magnetron sputtering. At two different discharge pressures of 0.6 and 1.2 Pa coatings with S/W ratio 0.6 – 1.6 were achieved with N_2 content 0 – 30 at. %. Nanostructured coatings with impregnated nano-crystallites WS_2 resulted in hardness up to 7 GPa with a discharge pressure of 1.2 Pa whereas higher hardness around 9 GPa was achieved at 0.6 Pa discharge pressure. Increasing the N content also increased in amorphousness in the coating. Coatings were tested tribologically in dry N_2 and humid air to compare the friction coefficients. In humid air, friction coefficient increased from ~ 0.2 – 0.3 with increasing N content. In dry N_2, average coefficient of friction was lower than 0.08 for all depositions and showed stable COF as compared to humid environment. Regardless of higher friction coefficient in moist air, the wear rate of coatings was almost similar for all N dopant percentages. However, the wear rate recorded in

protected dry N atmosphere was two times lower than wear rate measured in humid air which turned out to be about 1.5 x 10^{-6} mm^3 N^{-1} m^{-1}. It was deduced from Raman spectral analysis of nano-crystallites on ball wear scar that these nanograins of oxides are mainly responsible for spike in friction coefficient in humid environment, however, these delaminated areas are regularly replenished by transferred tribofilm from the underlying coating.

CHAPTER 3

3. EXPERIMENTAL PROCEDURE

3.1. Deposition Process

W-S-N coatings with increasing N concentration were produced by sputtering in a Hartec deposition chamber having 2 magnetrons positioned at 90 degrees in relation to each other. A tungsten disulphide (WS_2) target was mounted in cathode 1, whilst, in cathode 2 a chromium (Cr) target was placed. Depositions were performed on 3 different fine polished substrates for distinct characterization analysis as shown in Table 1:

Table 1: Substrates used for individual characterization

Substrate	**Analysis**
Si wafers	Morphology
FeCrAly chips	Chemical composition, morphology, structure, hardness, thermal stability
M2 steel (Ø25 x 7 mm)	Adhesion and tribological properties

Emery papers from P180 down to P1200 grit sizes were used to polish M2 steel substrates followed by fine polishing using diamond paste on steel cloth with 3 µm mesh size and lastly, 1 µm. Before placing substrates in the deposition chamber, they were sonicated in acetone for 15 minutes and then in ethanol for same period followed by drying in hot air. Samples were then fixed into the rotating substrate holder positioned at the centre of the chamber. The distance of the specimens to the target was 10 cm and during depositions the substrate holder rotated at 18 rpm.

Prior to the depositions, chamber was evacuated down to a pressure of 8.6×10^{-4} Pa. The targets were then sputter cleaned. At the same time, the substrates were etched as follows: i) Cr target powered with 500 W was sputter cleaned for 20 minutes while the substrates were etched by applying 240 V at substrate. The shutter was positioned in front of Cr target to avoid deposition of this material on the substrates ("deposition pressure" was 0.3 Pa),

ii) the shutter was moved for the front of the WS_2 target and target was powered with 350 W for cleaning at the same time that a bias of 160V was applied to the substrate for etching. After cleaning, an adhesion and a gradient layer were deposited to ensure the good adhesion of the films to the substrate. The Cr interlayer was produced by applying 1200 W at the Cr target and a substrate bias of 60V at the substrates for 5 min (deposition pressure was 0.3 Pa). After that the power applied at the Cr target was progressively reduced from 1200 to 0 at a rate of 200 W/min, whilst the WS_2 target was set to 350W since the beginning of the gradient layer. In the last minute of gradient layer deposition, nitrogen gas was introduced on the chamber. Final, WSN films were deposited without substrate for 2 hours by keeping the power at WS_2 target constant (350 W) for all coatings while flow of N_2 gas varied from 0 to 20 sccm to achieve series of W-S-N coatings with different N content. For comparison purposes a reference WS coating, without N additions, was also produced. Table 2 and Table 3 shows the list of deposited coatings along with the more important deposition parameters.

Table 2: Key parameters used for etching, cleaning, gradient layer and interlayer deposition

Steps		**Conditions at target (W)**			**Conditions at substrate (V)**			**Pressure (mbar)**	**Ar/N_2 flow (sccm)**	**Time (min)**
		Power (W)	Bias (V)	Current (I)	Power (W)	Bias (V)	Current (I)	P		
Cr Interlayer		1200	375	3.27	7	60	0.1	0.3	21.9 / 0	5
Gradient layer	WS_2 target	350				60		0.5	21.9 / 0	5
	Cr	1200 - 200								

Table 3: Key parameters used for Coatings' deposition with increasing N content

Steps	**Conditions at target (W)**			**Conditions at substrate (V)**	**Pressure (mbar)**	**Ar/N_2 flow (sccm)**	**Time (min)**
	Power (W)	Bias (V)	Current (I)	Substrate bias			
WSN0	350	830	0.4	0	0.5	21.9 / 0	120
WSN5	350	830	0.4	0	0.5	21.9 / 5	120

WSN12.5	350	830	0.4	0	0.5	21.9 / 12.5	120
WSN20	350	830	0.4	0	0.5	21.9 / 20	120

spectroscopy (WDS-Oxford Instrument) at an accelerating voltage of 15 kV. Surface and cross section morphologies were obtained through field emission scanning electron microscopy (SEM Zeiss Merlin) at different magnifications. Thickness of the coating, including the interlayer and gradient layers was obtained through cross-section imaging. X-ray diffraction (XRD using Philips X'PERT diffractometer) under grazing scan with the incident Cu $K_{\alpha 1}$ radiation $\lambda = 1.5406$ Å at an incidence angle 3° and a step size of 0.025 was utilised for crystal structure study.

Hardness and young's modulus of the coatings were determined by nanoindentation using a Berkovich pyramid diamond indenter (Micro Materials Nano Test platform). Tests were performed both on Silicon wafers and FeCrAly at 2 different locations with a total of 32 depth sensing indentations and average was recorded by the software. 2 mN load was selected to minimize the effect the substrate as well as to produce an indentation depth less than 10% of coating's thickness. All the measurements were recorded in the ambient room temperature with dwell time of 30s. The adhesion of coatings was examined using scratch tester (CSM Revetest) on coated M2 steel substrates. The specimens were scratched using a Rockwell indenter of 0.2 mm tip radius at a speed of 10 mm/min where load was progressively increased from 5-45 N at a loading rate of 100 N /min. Adhesion of coating was quantified in terms of critical loads by analysing scratches under an optical microscope and comparing L_{c1}, L_{c2} and L_{c3} for corresponding loads. L_{c1} is the first coating cracking, where on the initial part of scratch track chevron marks are formed as coating is distorted plastically, L_{c2} is the first coating chipping where first adhesive chipping initiates from the fringes, and L_{c3} stands for the 3rd critical load where more than 50% of the substrate is exposed.

Frictional behaviour of W-S-N coatings was studied through sliding reciprocating tribometer (SRV friction and wear apparatus). Round M2 steel coated specimens were used against 100Cr6 steel ball of 10mm diameter under reciprocating sliding conditions. Prior to testing, both the specimen and steel ball were sonicated in acetone and ethanol, 5 min in each. Tests were performed at 25 °C (RH ~ 35 – 45%) and 200 °C for 60000 cycles with test conditions: 20 min (1200s) test time, 10 N load, 2mm stroke size and 25 Hz frequency

resulting in 180m sliding distance. For every W-S-N coating, 3 tests were performed to ensure the reproducibility of results. Friction coefficient was continuously recorded during the tribological tests.

2D profilometer was used to take the wear profiles from 3 different regions of the wear scar. Profilometer readings were treated using Origin software to plot 2D profiles of wear track and calculate the area of material removed. Following formula was used to calculate the specific wear rate:

$$k\ ({}^{mm^3}/_{N.m}) = \frac{Volume\ of\ wear\ track\ (mm^3)}{Load\ (N) x\ sliding\ distance\ (m)} = \frac{A.l}{L.S}$$

Where, k is the specific wear rate, A is the area of wear track in mm^2, l is the length of wear track in mm, L is the applied load in N and S is the total sliding distance in m [46].

Thermal stability of the coatings was assessed at 200 °C and 400 °C in in hydrogenated argon atmosphere in furnace. The specimens were then placed inside a tube and the tube was placed inside of a furnace. Connected to the tube was a vacuum system which allowed to vacuum down the pressure inside to 10^{-4} Pa. For annealing treatment, a continuous flow of protective gas (Ar + H) was introduced up to reach a pressure of 0.5 Pa. To reach the desired annealing temperature a ramp rate 20 °C / min was used then annealing was carried out for 3 hours. Subsequently, annealed coatings were subjected to chemical composition, morphological, structural, and mechanical properties characterization and compared with the as-deposited ones.

CHAPTER 4

4. RESULTS AND DISCUSSION

4.1. Chemical composition & deposition rate

Chemical composition of WSNx coatings with increasing nitrogen measured by WDS is given in Table 4. It was noted that S/W ratio of reference WSN0 coating was less than the stoichiometric WS_2 compound.

Table 4: Chemical composition of WSNx coatings and deposition rate

Coating	N_2 flow (sccm)	Composition at. %				S/W	Deposition rate (nm / min)
		W	S	N	O		
WSN0	0	32.9	48.9	0.5	12.1	1.5	17.3
WSN5	5	33.5	39.4	12.6	9.3	1.2	20.3
WSN12.5	12.5	34	33.5	19.5	7.5	1.0	18.1
WSN20	20	31.5	33.6	21.9	8.6	1.1	17.7

Sulphur depletion is reported in the literature to be attributed to several factors, such as: preferential resputtering of sulphur atoms by reflected Ar neutrals and because of the higher mass of tungsten than sulphur and re-sputtering of S by Ar^+ ions bombardment [38], [40]. Indeed, although no bias was applied on the depositions there are always a self-bias which accelerates the Ar^+ ions which can bombard the growing film with high energy [47]. *Nossa et al.* [61], reported S/W ratio for pure coating deposited by r.f magnetron sputtering equals to 1. 9. As opposed to her research, re-sputtering of sulphur has been higher in these depositions since S/W ratio calculated in this work is just 1.5. Increasing the N concentration in the films decreased the S/W ratio in the coatings (1.5 to 1.1). Similar tendency was again reported by *Nossa et al.* for the same coating system, where the S/W ratio decreased from 1.9 to 1.3. *Mutafov et al.* [45] however reported similar S/W ratios with 1.2 Pa partial pressure as the coatings produced on this thesis with 0.5 Pa. The decrease of S/W ratio on the coatings with increasing N additions has been reported to be caused by the: poisoning of the WS2 target which affects the sputtering yield of S, additional N atoms hitting the coating resulting in preferential resputtering of S atom, and/or higher affinity of W to N over S [38], [47]. All the coatings displayed a considerable

concentration of oxygen on their chemical composition. Oxygen contamination can be attributed to oxygen atoms adsorbed on chamber wall which are released during deposition. On the other hand, although a high purity target was used on the depositions, due to the porous nature of WS_2 material, oxygen may have been incorporated in the target when it was exposed to the atmosphere air and release during depositions. The usual porous nature of the pure TMD coatings could also contribute to the incorporation of O on the film when exposed to the ambient air. Indeed, due to the porous nature of such type of pure films O can diffuse inwards the film and connect with W. The increase of N concentration on the films led to a slight decrease of the O amount on their composition. This is probably due to the repeated usage of the target which allows the continuous release of the trapped oxygen on the target and as will be seen latter due to the more compact nature of the N rich films which avoid the penetration of O when exposed to ambient air [38], [47].

Table 4 shows the deposition rate of the different coatings. The reference WSN0 coating showed the lowest deposition rate among all the coatings (17.3 nm/min). A spike in deposition rate was noticed with increasing nitrogen flow while depositing WSN5 coating. Although, it would be expected a decrease of deposition rate due to the poisoning of the target with N flow additions, the additional material being deposited contracted the loss of deposition rate, even despite of the increase of the compactness level of the film, as will be shown latter. The further increase of N concentration in the films, decreases the deposition rate of the films due to : i) the further increase of poison level of the target surface [48] and (ii) reflected Ar, N and Ar^+ ion bombardment induces re-sputtering of incoming species along with densification of coating surface making it difficult to grow vertically, hence, decreasing the deposition rate [47].

4.1. Thickness and morphology

Surface and fractured morphologies along with thickness of WSNx coatings were analysed using scanning electron microscopy (SEM – Zeiss Merlin). After obtaining micrographs, ImageJ was used to gauge the thickness of interlayer, gradient layer, coating, and total film. The thickness of the different layers and total thickness of the films are shown in table 5.

Table 5: Effect of N_2 flow on the coating thickness of as deposited coatings

	Thickness			
	Gradient layer (um)	Interlayer (um)	Final coating (um)	Total (um)
WSN0	0.6	0.4	1.1	2.1
WSN5	0.6	0.4	1.4	2.4
WSN12.5	0.6	0.4	1.2	2.2
WSN20	0.6	0.4	1.1	2.1

As expected, the thickness of the films follows similar trend as deposition rate shown in Table 5. For the reference WSN0 coating, the thickness achieved is in coherence with the work of *Yaqub et al*. [49] who managed to obtain 2.3 um coating thickness for pure $MoSe_2$ coatings (different TMD system but with similar thickness) deposited by DCMS technique what can be related to the porous, loose, and less compact structure as explained in his work. A compact 2 µm coating was achieved with up to N at. 21.8% as opposed to the work of *Fredrik et al.* [42] where he deposited films of 2.3 um thickness for N at. 34%.

In Fig. 3 (a and b), the reference WSN0 coating exhibited dense but columnar microstructure with upward extended vertical columns from the substrate to the coating surface. The surface morphology displayed a cauliflower like surface morphology, typical of pure TMD coatings. Under low mobility conditions the atoms stay at arriving positions.

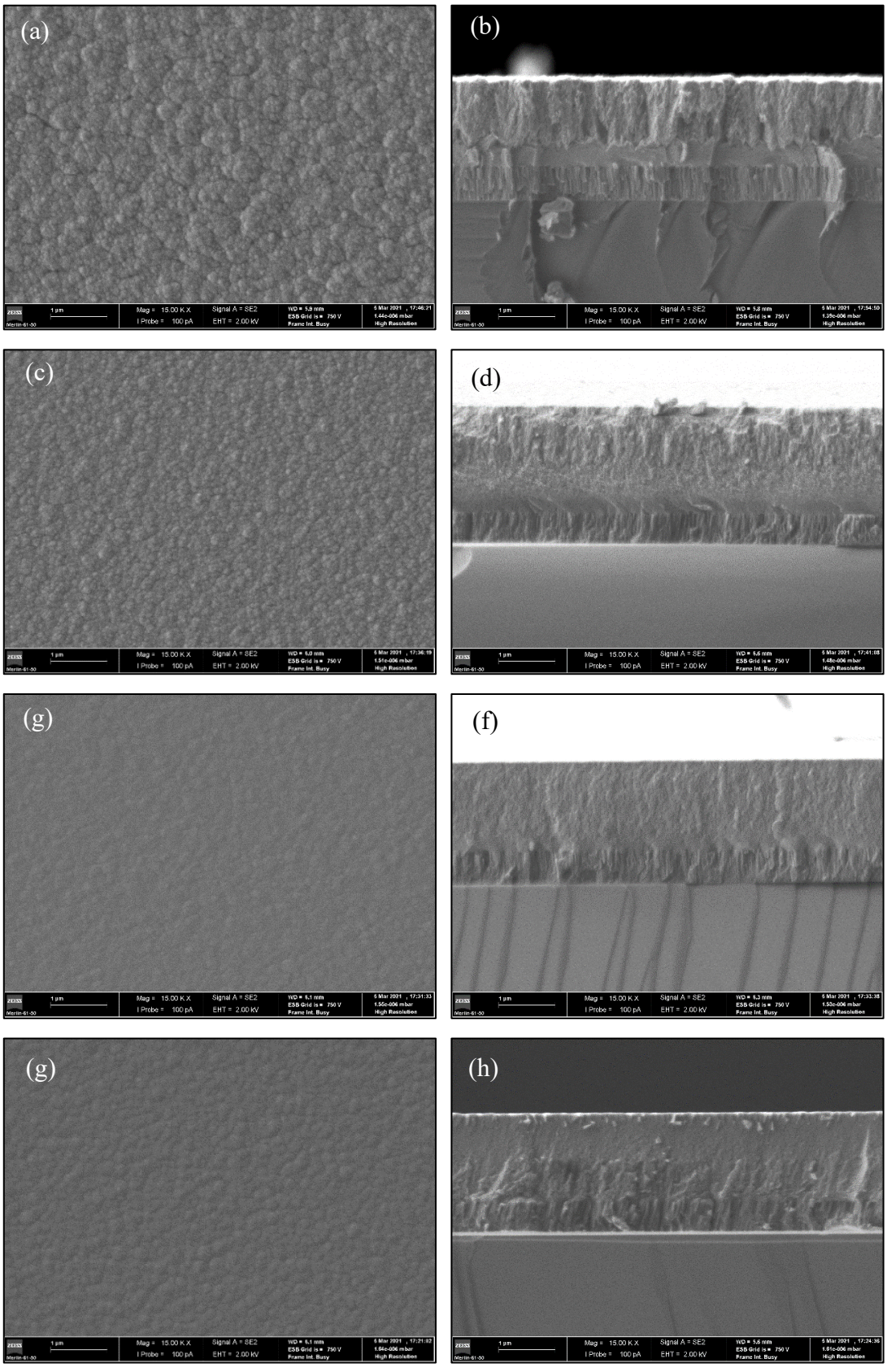

Figure 3: SEM micrographs of surface and cross section morphologies of as deposited a) and b) WSN0, c) and d) WSN5, e) and f) WSN12.5, g) and h) WSN20, coatings, respectively

With the film growing the adatoms will be preferentially captured at the top of the hills, resulting in rough surfaces and consequently to the growth of columnar structures. The porous morphology has been reported as a result of films growing under limited surface diffusion conditions leading to unstable growth [50]. The typical morphology of the pure TMD coatings, including WS coatings is sponge-like with much higher porosity than the one observed in this work. The reason for this may be the low S/W ratio of this films which is known to induce coatings compactness. As displayed in Fig 3. (c, e, and g), increasing the nitrogen concentration on the W-S-N coatings promotes progressive densification of the films microstructure and vanishing of the columnar growth. As referred previously, this densification together with the poisoning of the target influences the final thickness of the films. Additionally, cross-sectional SEM scan in Fig. 3 (b, d, f and h) shows that gradient and interlayer thickness stay same regardless of N concentration, but coating thickness reduces after 12.5 % N. Morphologies displayed in Fig. 3 agree with the previous studies on TMD-C(N) sputtered coatings deposited by *Nossa et al.* [40].

It can be thus concluded that N additions allows to produce more compact coatings. With that being stated, less porous morphology of N doped coatings, makes oxygen penetration from ambient air difficult, justifying the lower O concentration on N rich films.

4.1. Structure

XRD diffraction patterns of as-deposited films are shown in Fig. 4. Reference WSN0 coating displayed a strong characteristic pattern of WS_2 nano-crystalline films with visible diffraction peaks at 2θ position ~14°, in the range of 30 - 45°, ~60° and ~73° degrees. According to *Mutafov et al.* [45] the asymmetric peak with elongated shoulder on right in the 2θ range from 30 - 45° is indicative of series of 10L planes from single layers. This asymmetry arises from the turbostratic stacking of hexagonal planes of WS_2 which are rotated relevant to each other and referred to as 10L (L = 1, 2, 3, …) and (100). He also stated that with the increase of N content reflection of (002) plan prevails over other orientations.

For nitrogen doped WSNx coatings only (002) plane is prevalent at ~14°, however, with increasing the N concentration up to 22 at. %, the diffraction peaks shift towards lower

diffracting angles. The peaks shift towards lower diffracting angles is influenced by progressive low S/W ratio for N doped coatings since, there may be interstitial N in the structure which cause distortion in the lattice structure.

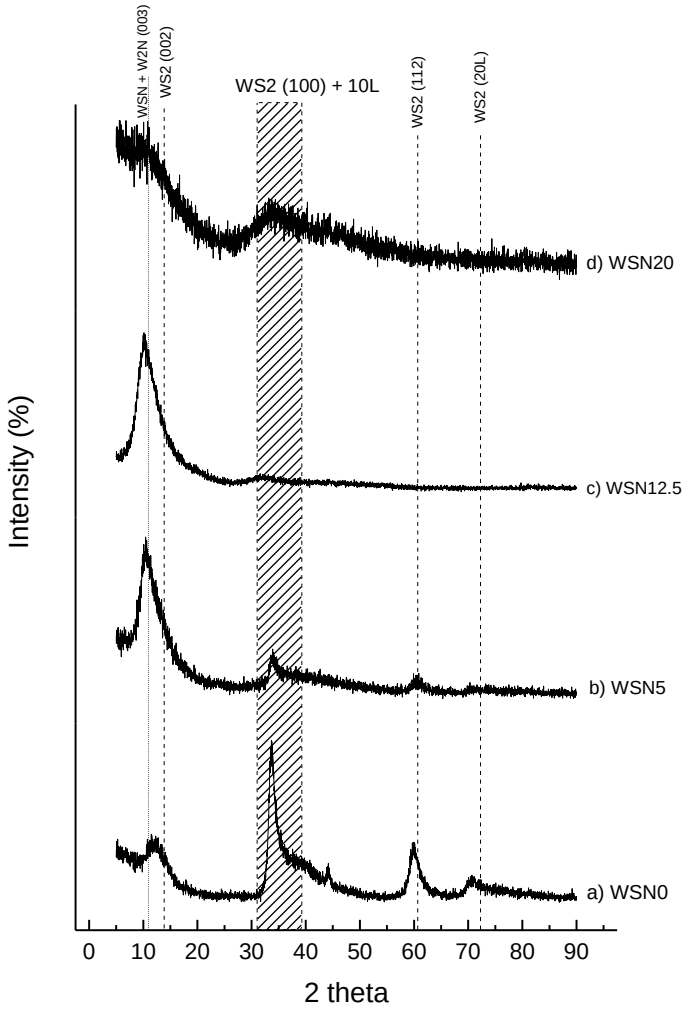

Figure 4: XRD diffractogram of as-deposited coatings

In addition to the metastable W-S-N phase which may be formed, the formation of W_2N crystallites, as indexed in the XRD diffractogram, also contributes to the diffraction peaks shift and broadening.

Additionally, with increasing N content the peaks have plateaued with significant reduction in intensity as to merely come as a bump. It is because of decrease in crystallite size of WS_2 phase below 10 nm by adding N, which makes it impractical for XRD to detect crystal structure below this limit. Similar observations were recorded by other scientists for N rich

W-S films. In one of the studies of W-S-N coatings deposited by reactive magnetron sputtering it was observed that coatings with N higher than 30 at. %, demonstrated a significant decrease in crystallinity [42], as is the case of the coating on this work with ~21.8 at. % of N. Formation of basal planes in TMD coatings is reasoned by the increase in the mobility of dopant element. It was validated by *Lauwerens et al.* [51] who uncovered that (002) planes are favoured for low S/W ratio in MoS_x films prepared by pulsed magnetron sputtering.

4.1. Hardness behaviour and adhesion

4.1.1. Hardness

The hardness results of sputtered deposited W-S-N coatings measured by nanoindentation are shown in Table 6.

Owing to the loose columnar and porous morphology of reference WS coating, it displays the lower hardness -3.74 GPa and Young's modulus among all the specimens. *Sundberg et al.* [43], achieved hardness of pure WS_2 coatings around 2 GPa. This difference in hardness as compared to the reference coating deposited on this work can be explained by the difference S/W ratios on the coatings (In this case, we have achieved S/W ratio of 1.5 and Sundberg also achieved S/W ratio below 2 for all coatings). Hence. there is higher contribution of tungsten on hardness behaviour of the coating due to excess W in W-S system. *Nossa et al.* [46] also confirmed hardness of pure WS_2 coatings to be ~0.6 GPa in one of his studies of W-S-N films deposited by r.f magnetron sputtering. For other compositions of W-S-N coatings, the hardness values were significantly improved with N doping as can be seen in Table 6. This rapid increase can be due to following reasons [45]:

(a) Increase in density of films with increasing N content. As shown in figure 3, N doped films are more compact and with fewer voids and pores. The slight decrease in hardness value for the coating with higher N concentration can be related to the amorphous character of the film, as displayed the XRD diffraction partner of this film in Fig. 4.

(b) With increasing N, the formation of hard WSN/W2N phases also increase the hardness of films.

(c) (002) preferential orientation in N doped systems as compared to (100) for reference coatings. When basal planes are aligned perpendicularly to the loading direction during the test it leads to most intense tensile stress field components aligned parallel to the surface under the indenter, which has stronger chemical bonds, hence, high hardness.

Previous research has shown that N doped coatings are harder than C doped systems [38]. Elastic modulus also increases with increasing N content due to the strong bonding energy promoted by the addition of N. Table 6 depicts that all N doped coatings showed higher H^3/E^2 ratio (~ 0.4 -0.7) as compared to reference WS coating (0.011) indicating that N rich coatings should display better fracture toughness.

Table 6: Mechanical properties of the as deposited coatings

Coating	Hardness (GPa)	Young's modulus (GPa)	H^3/E^2
WSN0	3.7	69.5	0.011
WSN5	6.6	73.5	0.054
WSN12.5	8.0	82.8	0.075
WSN20	7.2	96.0	0.041

4.1.1. Adhesion

Adhesion of the films to the substrate, evaluated by scratch testing is estimated by the failure mechanism of coating in terms of critical load values, nature of local spallation inside of the track, on the peripheral area and interfacial spallation.

Optical micrographs presented in Fig. 5 and critical load values shown in Table 7 shows an improvement in adhesive strength with increasing N percentage.

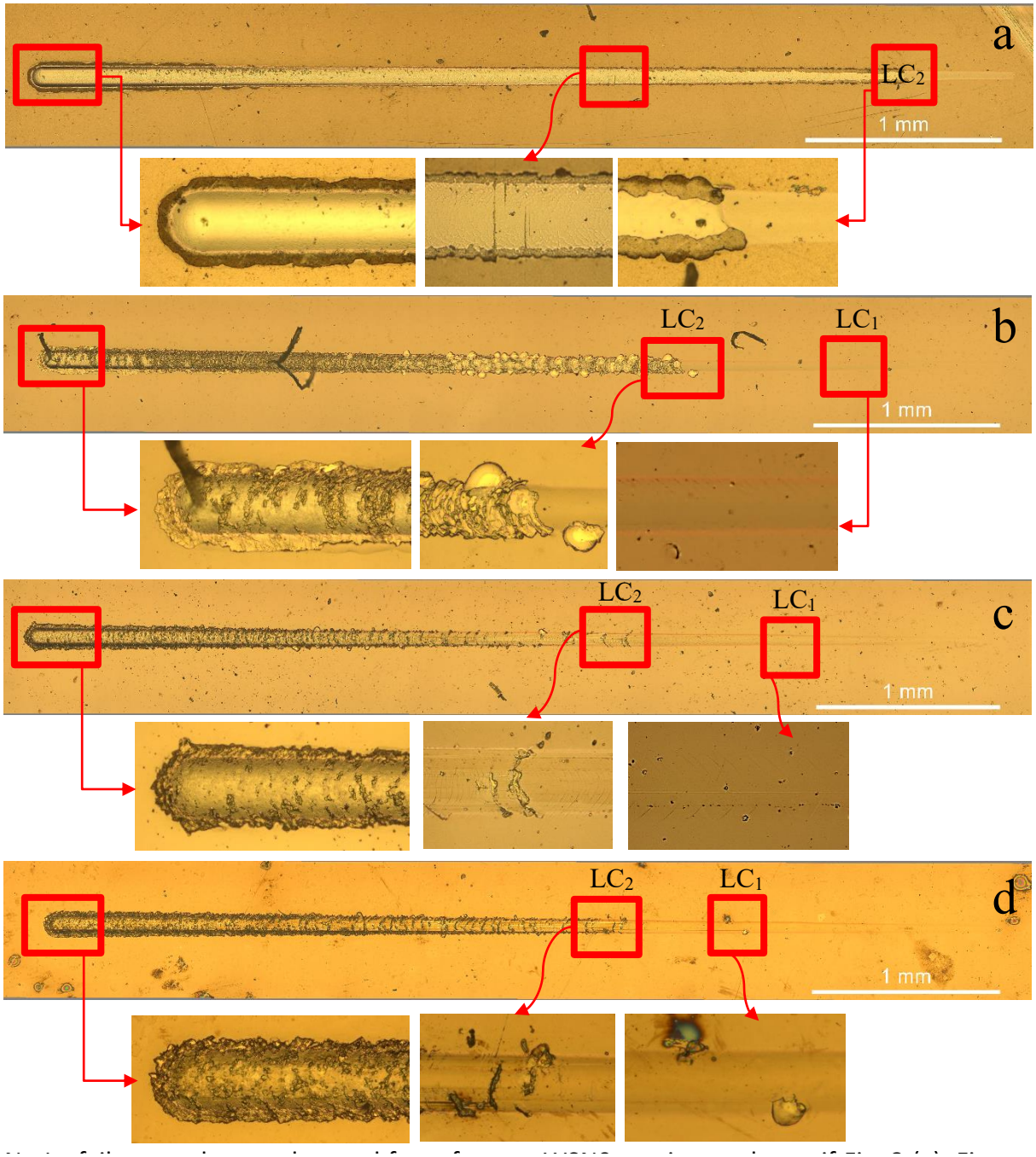

Figure 5: Typical Adhesion scratch tracks of as deposited coatings: (a) WSN0, (b) WSN5, (c) WSN12.5 (b), and (d) WSN20

soft nature of the pure WS_2 coating. No L_{C3} failure more could be observed on the reference film. For WSN5, Fig. 8(b) reveals that coating distorts plastically at 8N L_{c1} by making chevron rings followed by first chipping at 18N – described as $L_{C2.}$ Substrate was not exposed at any part of coating; however, local spallation was noticed inside which accumulated on the edges of track. Fig. 5 (c) shows that WSN12.5 has followed the same trend with increased Lc_1 endurance at 10N. Initial adhesive chipping was recorded at L_{c2} 21N which is significantly

higher as expected by keeping up with the previous test's performance of WSN12.5. Initial failure for WSN20 is presented in Fig. 5 (d) was observed at L_{c1} ~ 16N as chevron marks initiates from this point. One thing to be noted here is that a minor local chipping was noted on the bottom edge of track, which was not continuous for longer distance, so it was categorized as L_{C1}. Lc_2 was noted at 20.5 N load.

Table 7: Critical adhesion load for as deposited coatings

Coating	WSN0	WSN5	WSN12.5	WSN20
LC1	-	8 N	10 N	16 N
LC2	9.5 N	18 N	21 N	20.5
LC3	-	-	-	-

Surprisingly, none of the coatings has shown Lc_3 justifying good film-substrate adhesion and promising for tribological testing. As opposed to the results obtained for coatings deposited through dc sputtering by *Mutafov et al*. [45], where N at. % ranged from 0 – 30 at. % and the corresponding Lc_2 was 14N whereas in our research it is 6.5 N higher ~20.5.

These results are coherent with the study of *Mutafov et al.* [45], who stated that doped TMD films have proven to increase the adhesion of coating as the crystallinity is changed in the system as well as coating density. When N is preferentially sputtered along with the WS_2 target, the affinity of tungsten with nitrogen increases compared to with sulphur. Coating becomes harder due to W-N bonds and featureless compact morphology resists delamination of the system.

4.2. Tribological behaviour

Tribological performance of W-S-N coatings was evaluated in terms of coefficient of friction, wear rate and wear track investigation.

4.2.1. Coefficient of friction at room temperature

Friction coefficient evolution of coatings tested at room temperature are presented in Fig. 6 below, for which mean COF are 0.90, 0.12, 0.97, and 0.98 for W-S-N coatings with WSN0, WSN5, WSN12.5 and WSN20, respectively. WSN0 exhibits the lowest average COF ~0.9 among all the other coatings, in good agreement with other works on WSN coatings [41].

This coating started to wear out after 820 seconds, with consequent progressive increase of the COF value. Despite of the low friction displayed by this coating their bearing capacity is limited because of their porous nature and low mechanical properties, which led to their easier worn out during tribological tests. Consequently, as it will be shown later the specific wear rate of the coating will be higher. Theoretically, pure WS_2 films can slide past each other almost without friction but practically, as deposited films are not in desired orientation even though sliding happens in the oriented and crystalline WS_2 tribolayer. Best possible properties are not achieved by pure aligned crystalline WS_2 coatings as it gets worn out quickly and do not sustain humidity attack. To achieve optimal performance a compact, smooth, and mechanically strong film is required that can facilitate the formation of tribofilm as well. With the addition of 3rd element (N in this case) density and hardness of W-S-N coatings showed a notable improvement and allowed the formation of WS_2 tribofilm. WSN5 has shown the highest mean COF ~0.12 value among the other coatings, however, the coating sustained the whole sliding duration without any signs of wearing out of the film. Additionally, fluctuations in the COF value throughout the test duration is visible. The optimal performance has been exhibited by WSN12.5 apart from mean COF not very different from pure WSN0, the friction curve is stable and is evident of continuous supply of wear debris, WS rich, from coating for effective tribolayer formation and shown the least wear rate as it will be shown later. WSN20 had failed as it reached interlayer and offered COF up to 0.98. Change in surface roughness, formation of W_2N phase and change in orientation of (002) plane which hinders the easy supply of tribolayer could be the reason for high and unstable coefficient of friction.

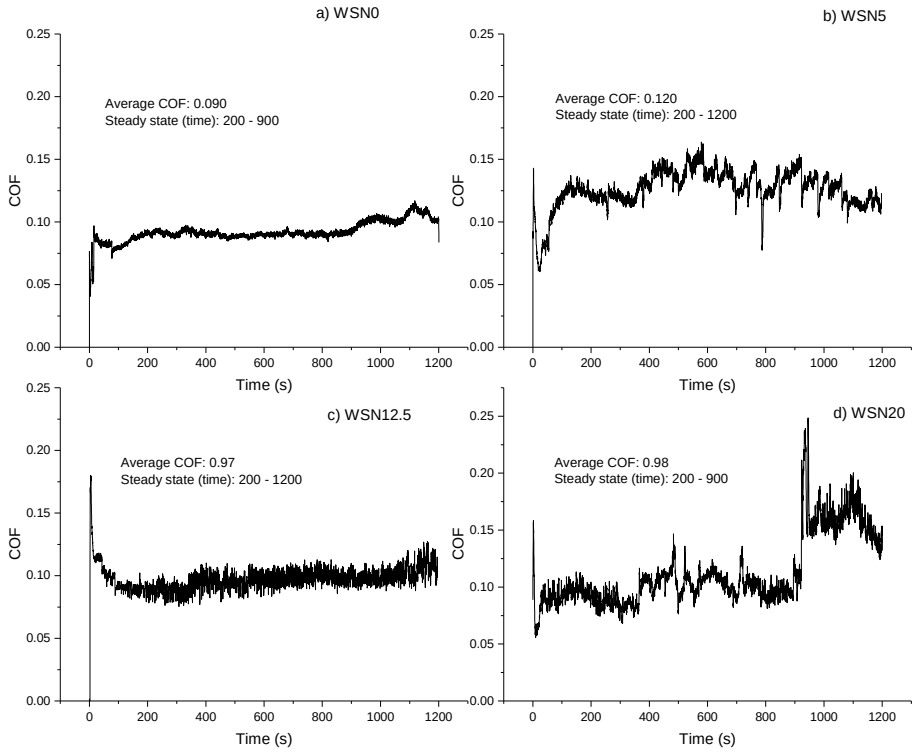

Figure 6: Fiction coefficients at room temperature for WSN films a) WSN0, b) WSN5, c) WSN12.5, d) WSN20

It is assumed that the basic principle for the easy formation of WS_2 is the ease of availability of individual constituents, i.e., W and S more than the need for aligned crystalline film itself. In sliding contacts, tribofilm is dynamic rather than static; since, the contact points of tribo-contact keep on shifting with time and gets removed from the system along with material transfer to the counterbody. Therefore, a continuous supply of stable lubricious tribofilm is required from the dense load bearing coating structure [42]. According to *Isaeva et al.* [44] diffusion of individual atoms is more beneficial in tribofilm formation than reorientation and movement of bigger W-S crystalline platelets. For Instance, amorphous W-S-N has proven to be good source for non-stop W and S supply when exposed to sliding environment and is facilitated by gaseous oxide of N, NO_x which gets removed from the system eventually. This is backed by the research carried out by Gustavsson who happened to obtain well aligned W-S tribofilm with N content higher than 34% [42]. Low S/W ratio allows more W to combine with N to form amorphous structure and is responsible for its good mechanical properties as well. As opposed to the research carried out by *Gustavsson*

et al. [42] in which he obtained 0.003 mean COF in dry N_2 sliding with 5000 cycles and 5N load in 10% RH we have managed to achieve well aligned tribolayer with 0.9 mean COF at 60,000 cycles with 10N load and 35% RH. For future, these coatings are to be tested under dry N_2. In case of WSN20, even though coating has shown almost same mean COF as WSN0 and WSN5 for steady state, but instantaneous COF went as high as 0.25 due to the film delamination.

Nitrogen is considered an astonishing addition for doping W-S films due to various reasons: (i) having gaseous oxides of N allows easy removal of N from contact facilitating tribolayer, (ii) in amorphous W-S-N structure, some percentage of N is present in its gaseous N_2 form and leaves the tribo-contact upon exposure, and (iii) W has high affinity towards N when present in excess amount but does not form hard and abrasive oxides (since oxides are gaseous). In conclusion, N_2 advantage over other elements is its easy removal from the tribofilm as well as amorphous W-N structure which results in dense coating with shearable continuous tribofilm [44].

4.2.1. Coefficient of friction at elevated temperature

Figure 7 demonstrates the frictional behaviour of W-S-N coatings at 200 °C under 10N load for 1200s (10 minutes & 60,000 laps). The mean COF values for the coatings are 0.047, 0.051, 0.034, and 0.028 for WSN0, WSN5, WSN12.5, and WSN20, respectively. As expected, the reported COF values for high temperature tests are much lower than room temperature tests mainly because of moisture removal.

Initially, WSN0 had achieved steady state after 100s (5000 laps) but then gradual rise in friction was observed. It is assumed that coating was worn out and reached interlayer, which is compact but not lubricious, therefore, has shown increase in COF after soft WS_2 coating (tribolayer) is depleted from the contact zone. The presence of hard ceramic WO_3 in the contact can be detrimental for tribolayer formation. WSN5 have exhibited highest mean COF among all test samples at HT. To choose the steady state from the fig. 10 (b) it is complicated since COF spiked in the beginning causing steady state to appear after 400s (20,000 laps). Tribotest for WSN5 did not touch the interlayer therefore wear rate is lower than WSN0 apart form highest COF values. WSN12.5 again shows the low COF among the coatings which backs up its justified N content to deliver good mechanical strength and

steady state tribological behaviour with low COF value. WSN20 provided the lowest friction coefficient (0.02).

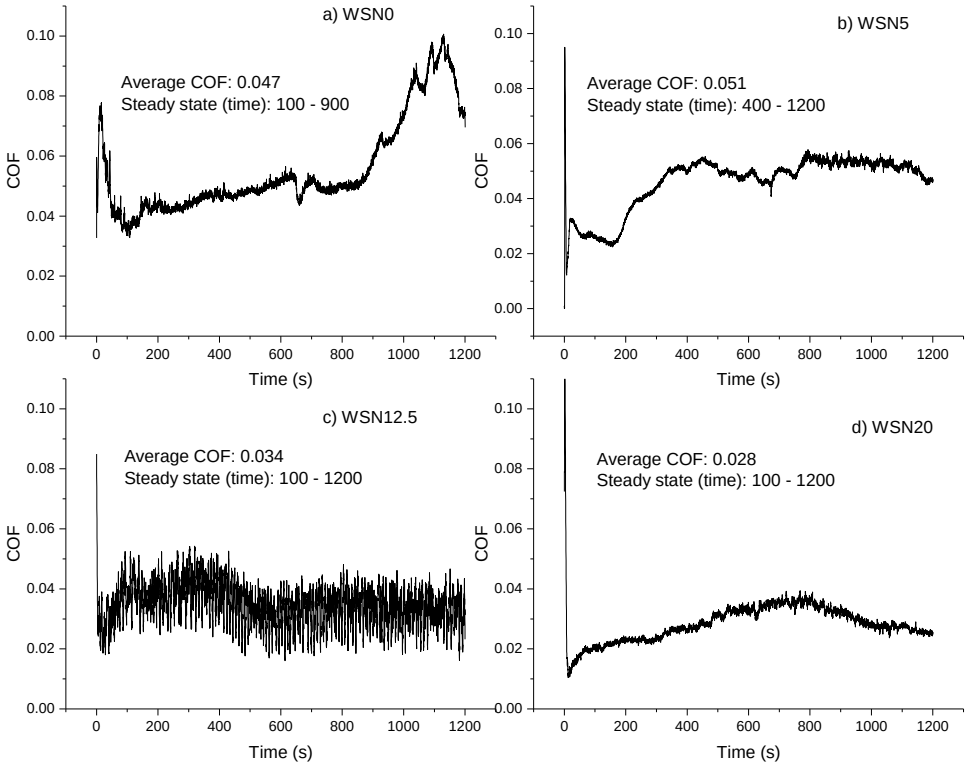

Figure 7: Friction coefficient at 200°C for WSN coatings: a) WSN0, b) WSN5, c) WSN12.5, d) WSN20

To sum up, all the coatings has shown significant drop in COF values as compared to room temperature tests. The moisture removal at elevated temperature is responsible for low friction of W-S-N coatings. Unlike pure WS_2 films, doped W-S-N coatings contain amorphous phases, i.e., WNS, WO_3 (most likely), and WN_x along with nanocrystalline WS_2. These dispersed phases throughout the structure cause dispersion strengthening of the coating which helps bear the load. Additionally, these dispersed nanocrystalline WS_2 phase are broken between friction pairs and reorients themselves in (002) preferential alignment. Due to weak Vander Waal's forces, these planes cause easy shearing hence we get load bearing and tribologically stable coating at high temperature (for instance WSN12.5) [52].

4.3. Wear track and counter body analysis

4.3.1. Room temperature

In Fig. 8, 2D profiles of these coatings are given along with wear tracks and ball images When sliding begins, initially worn coating gets aligned in the direction of sliding making tribofilm which is the key phenomena behind low COF. In Fig. 8, micrographs of 100Cr6 steel ball have demonstrated the adhered material on the surface of ball from the wear track. For WSN0, WSN5, and WSN12.5 counterbody wear is not observed except for WSN12.5.

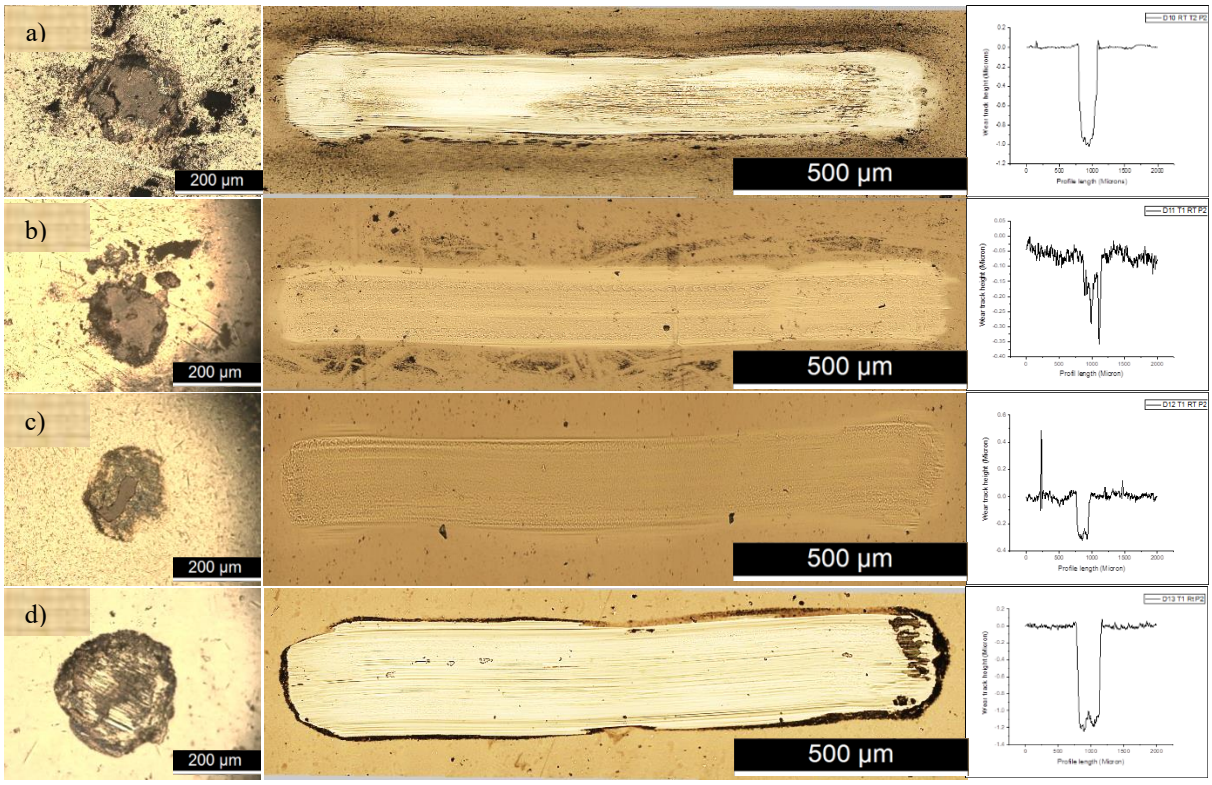

Figure 8: Optical micrographs of wear track and balls of SRV conducted at RT: a) WSN0, b) WSN5, c) WSN12.5, and d) WSN20.

As shown in Table 8, for pure WSN0 coating the specific wear rate is high which was expected as the morphology is rather loose with columnar and porous morphology and hence low load bearing capacity, so coating is depleted from the tribo contact constantly during sliding.

Table 8: Specific wear rate of coatings, wear and maximum depth achieved on the wear track of coatings tested at room temperature.

	WSN0	WSN5	WSN12.5	WSN20
Coating thickness (μm)	1.12	1.41	1.16	1.10
Average wear track height (depth) (μm)	0.96	0.38	0.40	1.31
Average specific wear rate (mm^3 / Nm)	4.61×10^{-7}	1.32×10^{-7}	1.01×10^{-7}	6.21×10^{-7}

Figure 8 c). shows that WSN12.5 coating has outperformed other coatings in terms of lowest specific wear rate ~ 1.01×10^{-7} (mm^3 / Nm) followed by WSN5 with k equals to 1.32×10^{-7} (mm^3 / Nm). However, tribotest for WSN20 has exhibited rather poor performance and WSN coating layer is removed from the system completely since it has exposed gradient layer. Poor performance of WSN20 can be attributed to the more amorphous character of the coating and presence of hard wear debris of W_2N on the track which may promote a more severe scratching of the wear track as shown in Fig. 9.

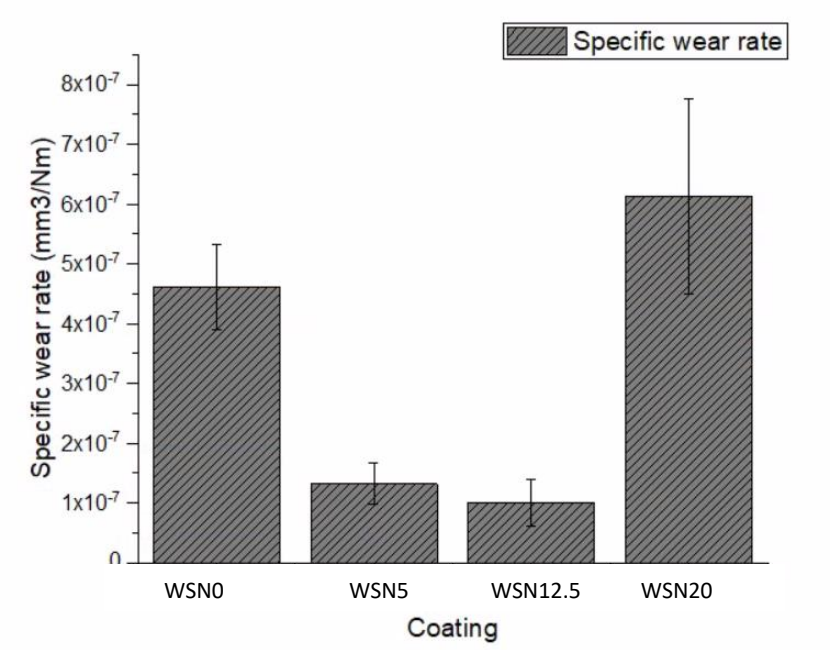

Figure 9: Specific wear rate of the coatings tested in ambient air at room temperature.

WSN12.5 wear track shows minimal wear residues and minimal adhered material on the surface of ball. So, 19.5 at. % N flow has proven to be the optimum dopant percentage in the depositions as it has high hardness as well as lowest wear rate with the formation of W-S tribofilm. The horizontal marks on the wear track represents crystalline aligned WS_2

tribofilm. These marks in Fig. 8 can clearly be seen for WSN0, WSN5, and WSN12.5 with minimum adhered material for WSN0, followed by WSN5 and maximum for WSN12.5. Whereas, for WSN20 the gradient layer was exposed and counterbody micrographs reveals that ball is worn to a certain extent with the adhered removed WS_2 layer. With increasing % N doping in the coating, the structure gets amorphous and featureless. Since tribofilm is formed by worn off coating when it reorients its (002) basal plane in the direction of sliding to offer low shear strength film responsible for reduced COF, the amorphous nature of doped coating will delay the reorientation of basal plane and formation of tribofilm. With WSN20 doped with highest ~22 at. % N, the amorphousness in the system also increases, so is the interaction with W to form W_2N and makes tribofilm phenomena difficult.

4.3.2. High temperature

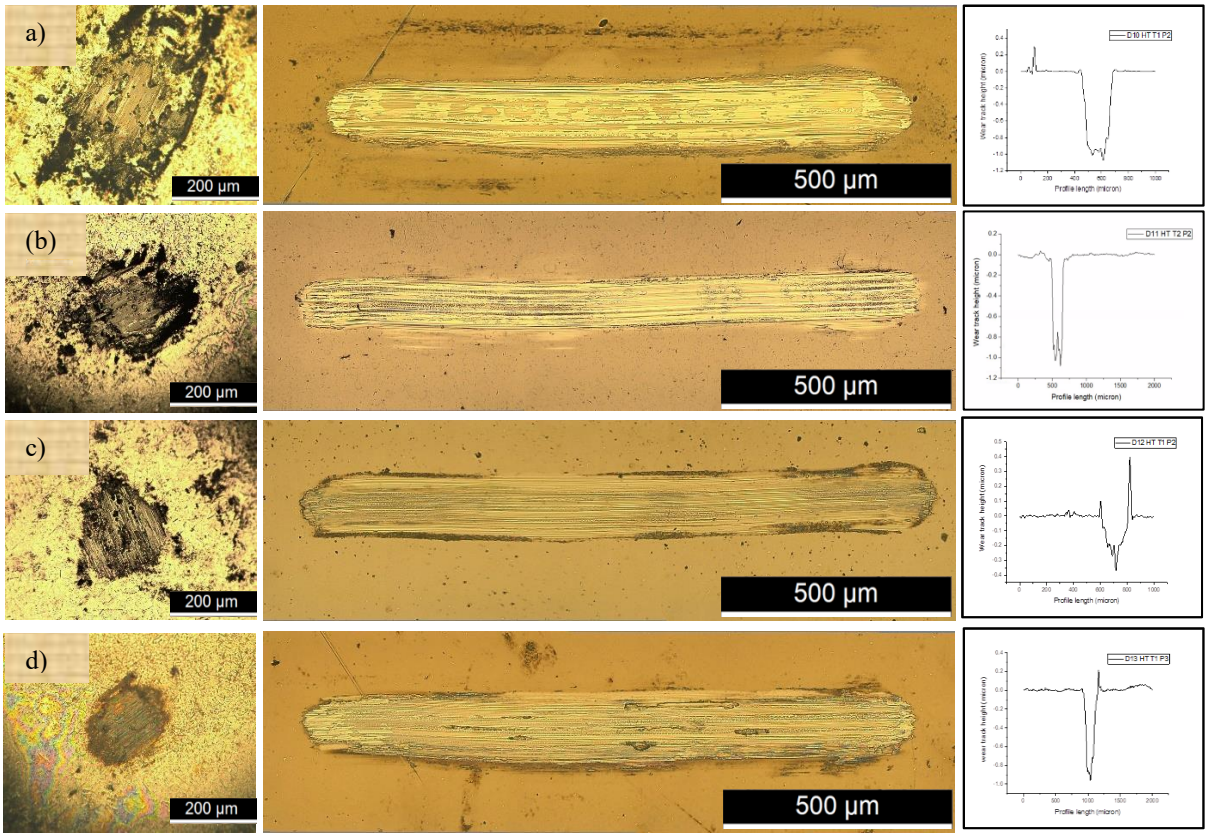

Figure 10: Optical micrographs of wear track and balls of SRV conducted at 200°C: a) WSN0, b) WSN5, c) WSN12.5, and d) WSN20.

In Fig. 10, wear tracks are shown for coatings tribologically tested at 200 °C for 20 minutes with test conditions same as the tests at room temperature: 10 N load, 25 Hz frequency

and 2 mm track length. As shown in the Table 9, WSN0 has exhibited highest wear rate among all coated samples due to its porous and soft nature. Wear rate for WSN5 is close to the wear rate obtained at room temperature tribo-test. WSN12.5 has again outperformed all coatings with its wear rate as minimum as 10^{-8}. WSN20 tested at high temperature also have shown a significant decrease in wear rate as compared to the ones tested at room temperature. Generally, compared with room temperature tribology tests it can be said that all coatings have performed better at high temperature testing since the wear resistance has substantially increased due to moisture removal.

Table 9: Wear rate and wear depth at high temperature

	WSN0	**WSN5**	**WSN12.5**	**WSN20**
Coating thickness (μm)	1.12	1.41	1.16	1.10
Average wear track height (μm)	1.05	1.1	0.5	0.9
Average specific wear rate (mm^3 / Nm)	2.93×10^{-7}	1.35×10^{-7}	7.24×10^{-8}	1.54×10^{-7}

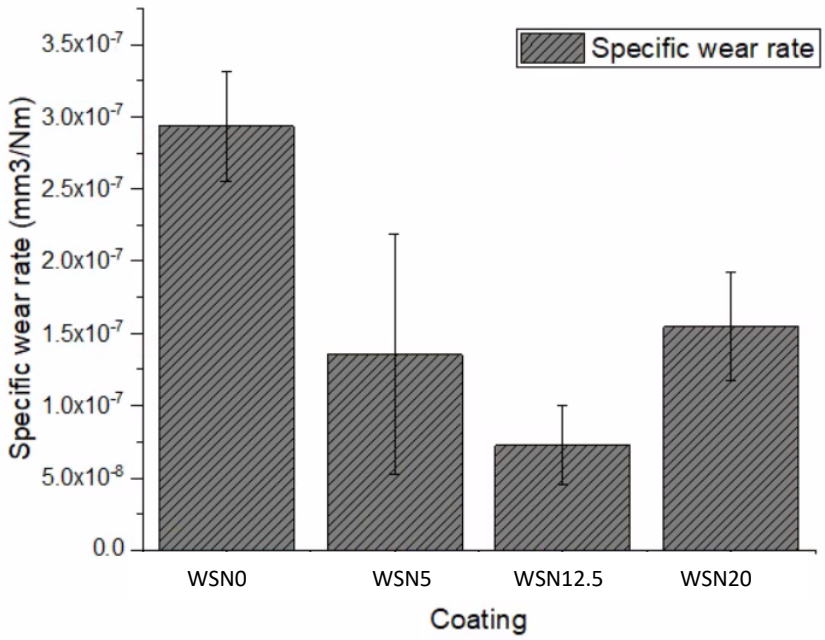

Figure 11: Specific wear rate of the coatings tested in ambient air at room temperature.

Previously, *Zhu et al. [*52] studied W-S-N coatings where obtained wear rate was 2.32×10^{-6} (mm^3/Nm) after testing at 200 °C for WSN (~17 % at. N) coatings deposited with magnetron sputtering. Contrarily, in this research we have obtained wear rate as low as 7.24×10^{-8} (mm^3/Nm) with WSN12.5 coating of wear track height only 0.5 μm.

Sundberg et al. [43] explained the reason for low wear in his work that absorbed water is removed from the surface at high temperature reducing the shear strength of film making transfer layer easier for the coatings. It can be seen in Fig. 10 that except WSN0, all balls have round transfer layer which facilitated low lubrication regime achievement. *Zhu et al.* [52] also explained that due to high temperature amorphous oxide particles are converted to crystalline WO_3. WO_3 crystals are then converted to friction pairs which reduces COF and wear rate of the coatings by obtaining lubrication system which is stable at high temperature.

4.4. Characterization after annealing

4.4.1. Chemical composition

Table 10 displays the chemical composition of all coatings before and after heat treatment in protective environment. As can be observed, chemical composition of coatings stays almost the same, except for O percentage which slightly decreased for all the compositions.

Table 10: Chemical composition of coatings before and after annealed at 200°C and 400 °C.

Coating	N_2 flow (sccm)	Composition at. %				S/W
		W	S	N	O	
WSN0	0	32.88	48.91	0.50	12.06	1.48
WSN0 (200°C)	0	34.86	50.85	0.026	4.89	1.5
WSN0 (400°C)	0	34.47	48.85	0.75	7.49	1.45
WSN5	5	33.50	39.44	12.59	9.29	1.17
WSN5 (200°C)	5	33.98	41.77	12.03	6.38	1.2
WSN5 (400°C)	5	33.34	38.88	11.95	7.84	1.16
WSN12.5	12.5	33.98	33.47	19.50	7.42	0.98
WSN12.5 (200°C)	12.5	35.87	36.10	19.01	3.86	1.0
WSN12.5 (400°C)	12.5	35.96	35.21	18.65	3.73	0.9
WSN20	20	31.49	33.59	21.87	8.59	1.06
WSN20 (200°C)	20	31.57	34.77	20.87	8.56	1.1

WSN20 (400°C)	20	32.67	35.16	21.02	5.39	1.07

4.4.2. Morphology:

In comparison of before annealed coatings, SEM micrographs of heat-treated coatings are given in Fig. 12.

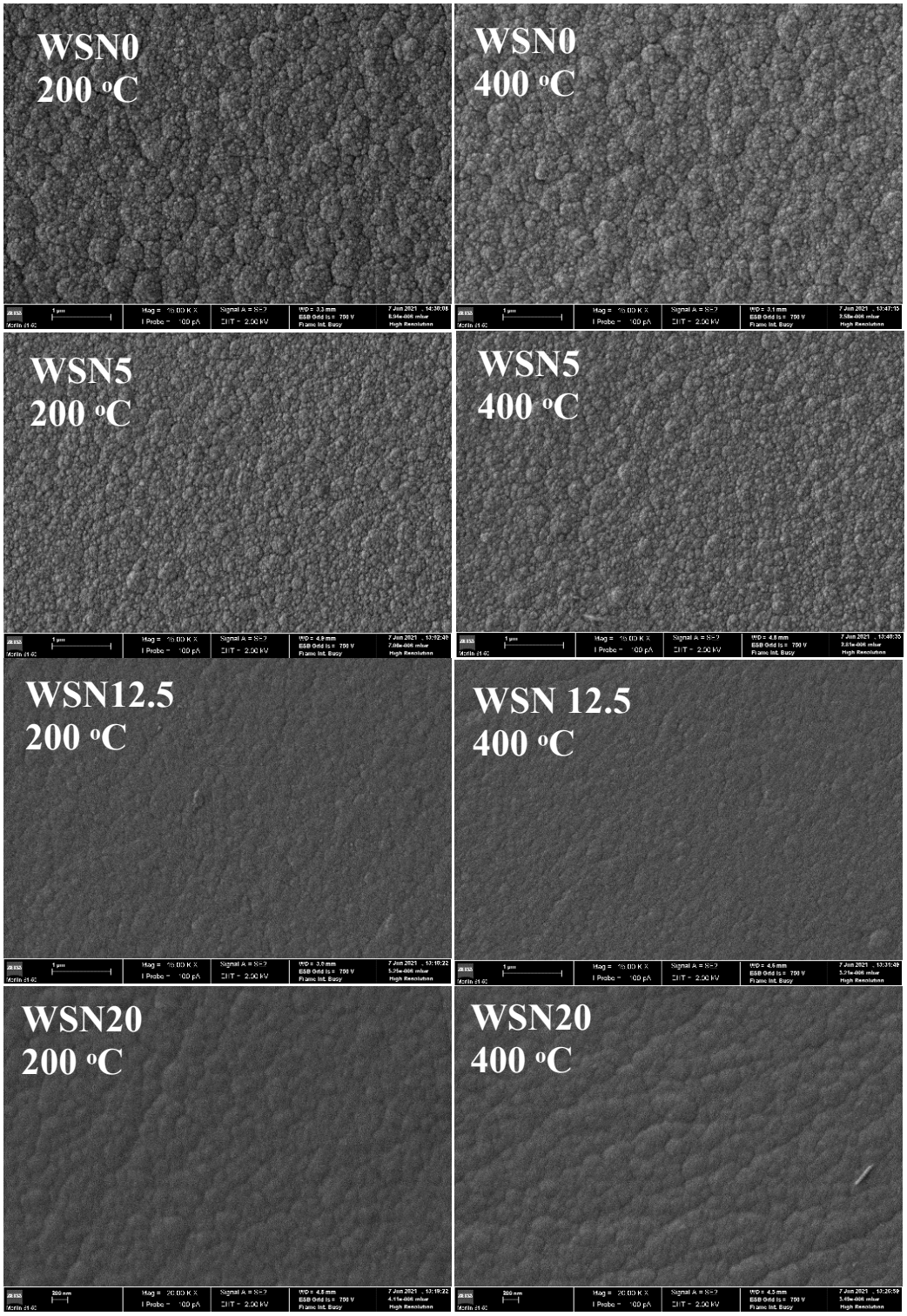

Figure 12: Surface morphology of coatings after annealing at 200 °C and 400 °C at 15kx magnification.

For WSN0, both temperatures did not cause noticeable change in the microstructure. Similarly, WSN5 also cannot exhibit noticeable changes on the surface closely packs grains. However, for WSN12.5 there is no clear morphology that was observed rather it seems even more compact than the before heat treated sample. Lastly, WSN20 is also compact as compared to WSN12.5 but not as big grains as in WSN0 and WSN5. It can be said that annealing has not changed the surface morphology of coatings. Cross-sectional morphology was not recorded due to some other tests that were yet to be performed on the sample so did not make it possible to cut the specimens for recording cross-sectional images of coatings.

4.4.3. Structure

Since the phases and position of the different diffraction patterns were defined already in Fig. 4, only comparison of individual coating diffraction patterns will be done in this section. Figure 13 shows the change in intensity of peaks of the coatings before and after annealing.

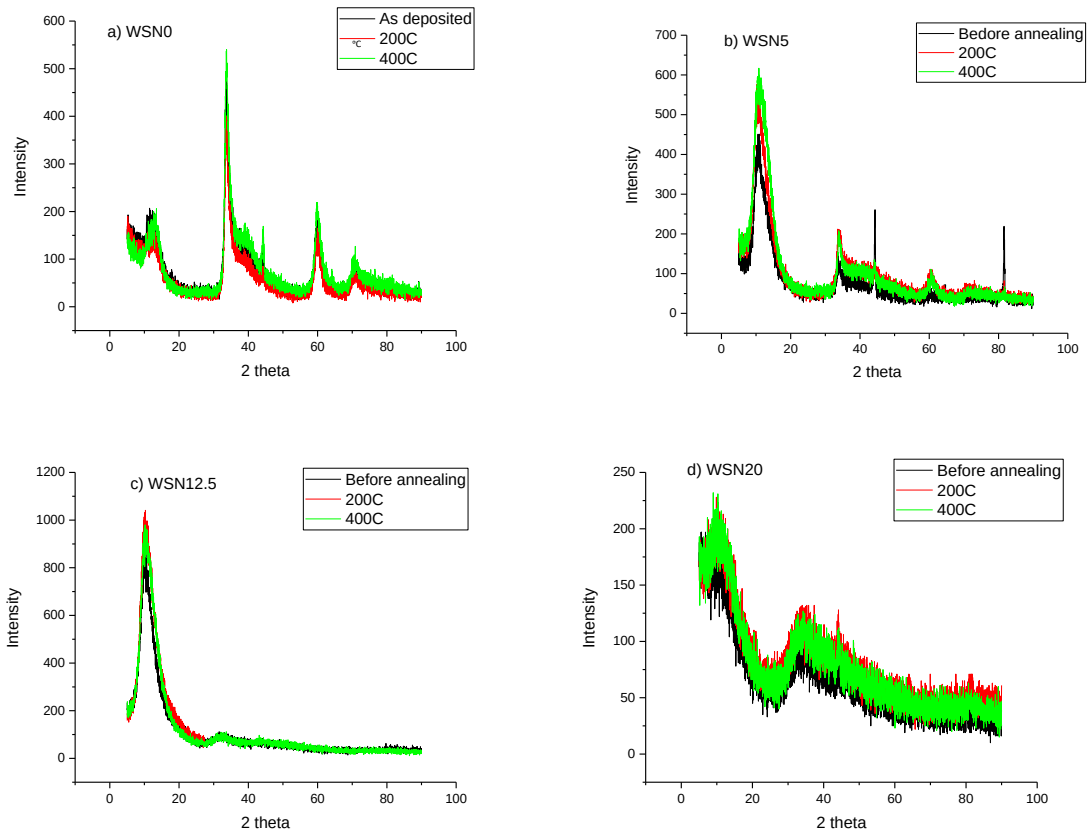

Figure 13: Individual XRD scan analysis for coatings after annealing at 200°C and 400°C: a) WSN0, b) WSN5, c) WSN12.5, and d) WSN20.

It is noticeable that the intensity of peaks for all compositions have increased a little after annealing at 400 °C making it more crystalline. For WSN5, two peaks were additionally noticed for un-annealed sample which is coming from the substrate. Since literature lacks data on the heat treatment of W-S-N and other TMD coatings so no comparison can be made so far to check the validity of tests. Since changes on the structure occurred, mechanical properties of the coatings were evaluated too.

4.4.4. Hardness of coatings

As opposed to other post annealing characterization results, hardness of the coatings has shown a noticeable change in values and has made coatings more load bearing.

WSN0 reference coating has shown a gradual decrease in the hardness values of the coatings because of crystallization of (002) plane in WS_2 which has made the coatings softer. For the rest of the coatings, hardness has only demonstrated increasing behaviour. However, the change in hardness is more noticeable after heat treatment at 400 °C. Among all the coatings, WSN12.5 has shown maximum hardness followed by WSN20, WSN5 and WSN0 in order as shown in Fig. 14. It can be concluded that hardness increase is associated with increasing crystallinity.

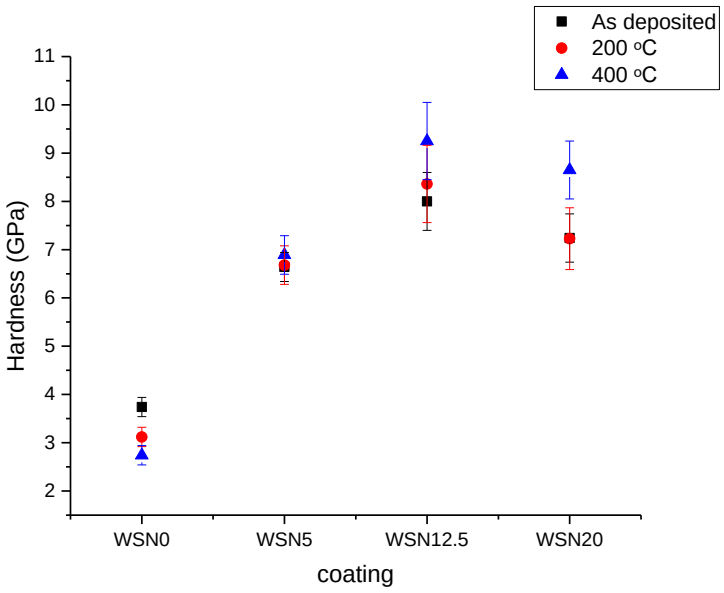

Figure 14: Hardness values comparison of as deposited and heat-treated W-S-N coatings

CHAPTER 5

5. CONCLUSION

W-S-N coatings with progressive increase of N concentration were deposited from a WS_2 target along with nitrogen gas flow in the chamber. The influence of N flow (sccm) on the properties of as deposited and heat-treated coatings was explored.

- Increasing N flow from 0 to 20 sccm led to increase nitrogen content in coatings from 0 at. % to 22 at. %. The maximum S/W ratio (in case of WSN0) obtained was 1.45 for both as deposited and heat-treated coatings and then it decreased with N addition due to high affinity of W towards N instead of S.
- Pure WSN0 coatings performed inadequately in terms of adhesion, hardness, and wear rate because of their loose and porous columnar morphology. Reference WSN0 coatings showed a crystalline structure, whereas with the increasing flow of nitrogen in the chamber coatings with higher concentration of N, such as WSN20 became X-ray amorphous. The presence of W-S-N phase in N rich coatings is not evident but W_2N phase could be indexed in the XRD diffractograms. N incorporation in the lattice structure with low S/W ratio have caused the shift in peak for N rich coatings.
- The hardness of coatings has evidently increased as the morphology became compact with nitrogen addition in the coatings with WSN12.5 being the highest in value. The coatings that were annealed displayed better hardness results in comparison to the as deposited coatings. This hardness increase of coatings during annealing is due to the increase of their crystallinity. W-S-N sputtered coatings displayed excellent sliding properties in comparison to literature with good coating adhesion and low wear rates.
- The tribological results obtained with low S/W ratio along with nitrogen doping were quite impressive and current study appeared to be the successful beginner step in upscaling the industrial applications for systems sliding in high temperature atmospheres.

- Thermal stability of coatings was evaluated by annealing in protective Ar atmosphere. As a result, annealed coatings showed no visible changes in the morphology and structure of the WSNx coatings. However, hardness values shows a noticeable increase after annealing at 400 °C.

CHAPTER 6

6. FUTURE WORK

The following future work is recommended for the systematic study of WSN coatings:

- Perform dry N_2 tribological SRV tests on as deposited coatings
- Anneal coatings further at 600 °C
- Perform cross sectional morphological SEM scan on annealed coatings of all temperatures (200 °C, 400 °C, and 600 °C)
- Carry out scratch tests on annealed coatings
- Perform hardness nano-indentation test on the coatings annealed at 600 °C.
- Perform tribological analysis on annealed coatings of all temperature in 3 different environments, i.e., room temperature, elevated temperature and dry N_2.

7. REFERENCES

[1] A. Sethuramiah, Ed., '1. Tribology in perspective', in *Tribology Series*, vol. 42, Elsevier, 2003, pp. 1–34. doi: 10.1016/S0167-8922(03)80004-4.

[2] F. Gustavsson and S. Jacobson, 'Diverse mechanisms of friction induced self-organisation into a low-friction material – An overview of WS2 tribofilm formation', *Tribol. Int.*, vol. 101, pp. 340–347, Sep. 2016, doi: 10.1016/j.triboint.2016.04.029.

[3] J. A. Tichy and D. M. Meyer, 'Review of solid mechanics in tribology', *Int. J. Solids Struct.*, vol. 37, no. 1, pp. 391–400, Jan. 2000, doi: 10.1016/S0020-7683(99)00101-8.

[4] T. Polcar and A. Cavaleiro, 'Review on self-lubricant transition metal dichalcogenide nanocomposite coatings alloyed with carbon', *Surf. Coat. Technol.*, vol. 206, no. 4, pp. 686–695, Nov. 2011, doi: 10.1016/j.surfcoat.2011.03.004.

[5] A. A. Voevodin and J. S. Zabinski, 'Supertough wear-resistant coatings with "chameleon" surface adaptation', *Thin Solid Films*, vol. 370, no. 1, pp. 223–231, Jul. 2000, doi: 10.1016/S0040-6090(00)00917-2.

[6] K. Holmberg and A. Erdemir, 'Influence of tribology on global energy consumption, costs and emissions', *Friction*, vol. 5, no. 3, pp. 263–284, Sep. 2017, doi: 10.1007/s40544-017-0183-5.

[7] M. de B. Bouchet, J. M. Martin, C. Matta, and L. Joly-Pottuz, 'The Future of Boundary Lubrication by Carbon Coatings and Environmentally Friendly Additives', in *Advanced Tribology*, Berlin, Heidelberg, 2010, pp. 598–599. doi: 10.1007/978-3-642-03653-8_193.

[8] M. Kalin, J. Kogovšek, and M. Remškar, 'Nanoparticles as novel lubricating additives in a green, physically based lubrication technology for DLC coatings', *Wear*, vol. 303, no. 1, pp. 480–485, Jun. 2013, doi: 10.1016/j.wear.2013.03.009.

[9] N. H. Forster, 'Rolling Contact Testing of Vapor Phase Lubricants—Part III: Surface Analysis©', *Tribol. Trans.*, vol. 42, no. 1, pp. 1–9, Jan. 1999, doi: 10.1080/10402009908982183.

[10] D. Berman and J. Krim, 'Surface science, MEMS and NEMS: Progress and opportunities for surface science research performed on, or by, microdevices', *Prog. Surf. Sci.*, vol. 88, no. 2, pp. 171–211, May 2013, doi: 10.1016/j.progsurf.2013.03.001.

[11] B. Bhushan, *Modern Tribology Handbook, Two Volume Set*. CRC Press, 2000.

[12] H. Cao, 'Self-adaptive and self-healing nanocomposite tribocoatings', 2019, Accessed: Jul. 24, 2021. [Online]. Available: https://research.rug.nl/en/publications/self-adaptive-and-self-healing-nanocomposite-tribocoatings

[13] E. Bergmann, G. Melet, C. Müller, and A. Simon-Vermot, 'Friction properties of sputtered dichalcogenide layers', *Tribol. Int.*, vol. 14, no. 6, pp. 329–332, Dec. 1981, doi: 10.1016/0301-679X(81)90100-6.

[14] J. Esteve, G. Zambrano, C. Rincon, E. Martinez, H. Galindo, and P. Prieto, 'Mechanical and tribological properties of tungsten carbide sputtered coatings', *Thin Solid Films*, vol. 373, no. 1, pp. 282–286, Sep. 2000, doi: 10.1016/S0040-6090(00)01108-1.

[15] A. Grill, 'Diamond-like carbon: state of the art', *Diam. Relat. Mater.*, vol. 8, no. 2, pp. 428–434, Mar. 1999, doi: 10.1016/S0925-9635(98)00262-3.

[16] G. Straffelini, *Friction and Wear: Methodologies for Design and Control*. Springer International Publishing, 2015. doi: 10.1007/978-3-319-05894-8.

[17] H. A. Jehn, 'Multicomponent and multiphase hard coatings for tribological applications', *Surf. Coat. Technol.*, vol. 131, no. 1, pp. 433–440, Sep. 2000, doi: 10.1016/S0257-8972(00)00783-0.

[18] A. Savan, E. Pflüger, R. Goller, and W. Gissler, 'Use of nanoscaled multilayer and compound films to realize a soft lubrication phase within a hard, wear-resistant matrix', *Surf. Coat. Technol.*, vol. 126, no. 2, pp. 159–165, Apr. 2000, doi: 10.1016/S0257-8972(00)00542-9.

[19] A. A. Voevodin, J. P. O'Neill, and J. S. Zabinski, 'WC/DLC/WS2 nanocomposite coatings for aerospace tribology', *Tribol. Lett.*, vol. 6, no. 2, pp. 75–78, Mar. 1999, doi: 10.1023/A:1019163707747.

[20] E. R. Braithwaite, *Solid Lubricants and Surfaces*. Elsevier, 2013.

[21] T. W. Scharf and S. V. Prasad, 'Solid lubricants: a review', *J. Mater. Sci.*, vol. 48, no. 2, pp. 511–531, Jan. 2013, doi: 10.1007/s10853-012-7038-2.

[22] K. Bewilogua and D. Hofmann, 'History of diamond-like carbon films — From first experiments to worldwide applications', *Surf. Coat. Technol.*, vol. 242, pp. 214–225, Mar. 2014, doi: 10.1016/j.surfcoat.2014.01.031.

[23] A. Erdemir, O. L. Eryilmaz, and G. Fenske, 'Synthesis of diamondlike carbon films with superlow friction and wear properties', *J. Vac. Sci. Technol. A*, vol. 18, no. 4, pp. 1987–1992, Jul. 2000, doi: 10.1116/1.582459.

[24] N. Takahashi, 'Direct resolution of the layer lattice of molybdenum disulphide by transmission electron microscopy in relation to lubrication', *Wear*, vol. 124, no. 3, pp. 279–289, Jun. 1988, doi: 10.1016/0043-1648(88)90218-9.

[25] J. M. Martin, 'Molybdenum Disulphide Lubrication: A.R. Lansdown, Tribology series, 35, D. Dowson (Ed.) 1999, pp. 380', *Tribol. Int.*, vol. 33, no. 2, pp. 148–149, Feb. 2000, doi: 10.1016/S0301-679X(00)00020-7.

[26] N. Onofrio, D. Guzman, and A. Strachan, 'Novel doping alternatives for single-layer transition metal dichalcogenides', *J. Appl. Phys.*, vol. 122, no. 18, p. 185102, Nov. 2017, doi: 10.1063/1.4994997.

[27] R. L. Fusaro, 'Lubrication and Failure Mechanisms of Molybdenum Disulfide Films', p. 31.

[28] V. Buck, 'Preparation and properties of different types of sputtered MoS2 films', 1987, doi: 10.1016/0043-1648(87)90116-5.

[29] V. Fox, J. Hampshire, and D. Teer, 'MoS2/metal composite coatings deposited by closed-field unbalanced magnetron sputtering: tribological properties and industrial uses', *Surf. Coat. Technol.*, vol. 112, no. 1, pp. 118–122, Feb. 1999, doi: 10.1016/S0257-8972(98)00798-1.

[30] J. M. Martin, H. Pascal, C. Donnet, Th. Le Mogne, J. L. Loubet, and Th. Epicier, 'Superlubricity of MoS2: crystal orientation mechanisms', *Surf. Coat. Technol.*, vol. 68–69, pp. 427–432, Dec. 1994, doi: 10.1016/0257-8972(94)90197-X.

[31] C. Donnet, J. M. Martin, Th. Le Mogne, and M. Belin, 'The origin of super-low friction coefficient of MoS2 coatings in various environments', in *Tribology Series*, vol. 27, D. Dowson, C. M. Taylor, T. H. C. Childs, M. Godett, and G. Dalmaz, Eds. Elsevier, 1994, pp. 277–284. doi: 10.1016/S0167-8922(08)70317-1.

[32] M. Suzuki, 'Comparison of tribological characteristics of sputtered MoS2 films coated with different apparatus', *Wear*, vol. 218, no. 1, pp. 110–118, Jun. 1998, doi: 10.1016/S0043-1648(98)00143-4.

[33] T. Onodera *et al.*, 'A Computational Chemistry Study on Friction of h-MoS2. Part I. Mechanism of Single Sheet Lubrication', *J. Phys. Chem. B*, vol. 113, pp. 16526–36, Dec. 2009, doi: 10.1021/jp9069866.

[34] K. H. Kannur, 'Optimization of nitrogen-alloyed Mo/W Sx Coating for low friction applications : state of the art', University of Coimbra, Coimbra, Portugal, 2018.

[35] P. D. Fleischauer, J. R. Lince, P. A. Bertrand, and R. Bauer, 'Electronic structure and lubrication properties of molybdenum disulfide: a qualitative molecular orbital approach', *Langmuir*, vol. 5, no. 4, pp. 1009–1015, Jul. 1989, doi: 10.1021/la00088a022.

[36] A. Nossa and A. Cavaleiro, 'Chemical and physical characterization of C(N)-doped W–S sputtered films', *J. Mater. Res.*, vol. 19, no. 8, pp. 2356–2365, Aug. 2004, doi: 10.1557/JMR.2004.0293.

[37] H. Liu and X. Zhang, 'Improved tribological properties of sputtered MoS2 films through N+ implantation', *Thin Solid Films*, vol. 240, no. 1, pp. 97–100, Mar. 1994, doi: 10.1016/0040-6090(94)90702-1.

[38] A. Nossa and A. Cavaleiro, 'Mechanical behaviour of W–S–N and W–S–C sputtered coatings deposited with a Ti interlayer', *Surf. Coat. Technol.*, vol. 163–164, pp. 552–560, Jan. 2003, doi: 10.1016/S0257-8972(02)00622-9.

[39] A. Nossa and A. Cavaleiro, 'Behaviour of Nanocomposite Coatings of W-S-N/C System under Pin-on-Disk Testing', *Mater. Sci. Forum*, vol. 455–456, pp. 515–519, 2004, doi: 10.4028/www.scientific.net/MSF.455-456.515.

[40] A. Nossa, A. Cavaleiro, N. J. M. Carvalho, B. J. Kooi, and J. T. M. D. Hosson, 'On the microstructure of tungsten disulfide films alloyed with carbon and nitrogen', 2005, doi: 10.1016/j.tsf.2005.02.018.

[41] A. Nossa and A. Cavaleiro, 'The influence of the addition of C and N on the wear behaviour of W–S–C/N coatings', *Surf. Coat. Technol.*, vol. 142–144, pp. 984–991, Jul. 2001, doi: 10.1016/S0257-8972(01)01249-X.

[42] F. Gustavsson, S. Jacobson, A. Cavaleiro, and T. Polcar, 'Ultra-low friction W–S–N solid lubricant coating', *Surf. Coat. Technol.*, vol. 232, pp. 541–548, Oct. 2013, doi: 10.1016/j.surfcoat.2013.06.026.

[43] J. Sundberg, H. Nyberg, E. Särhammar, T. Nyberg, S. Jacobson, and U. Jansson, 'Influence of composition, structure and testing atmosphere on the tribological

performance of W–S–N coatings', *Surf. Coat. Technol.*, vol. 258, pp. 86–94, Nov. 2014, doi: 10.1016/j.surfcoat.2014.09.061.

[44] L. Isaeva *et al.*, 'Amorphous W–S–N thin films: The atomic structure behind ultra-low friction', *Acta Mater.*, vol. 82, pp. 84–93, Jan. 2015, doi: 10.1016/j.actamat.2014.08.043.

[45] P. Mutafov, M. Evaristo, A. Cavaleiro, and T. Polcar, 'Structure, mechanical and tribological properties of self-lubricant W–S–N coatings', *Surf. Coat. Technol.*, vol. 261, pp. 7–14, Jan. 2015, doi: 10.1016/j.surfcoat.2014.11.074.

[46] A. Nossa and A. Cavaleiro, 'Tribological Behaviour of N(C)-Alloyed W–S Films', *Tribol. Lett.*, vol. 28, pp. 59–70, Jan. 2007, doi: 10.1007/s11249-007-9248-3.

[47] K. Hebbar Kannur *et al.*, 'Synthesis and structural properties of Mo-S-N sputtered coatings', *Appl. Surf. Sci.*, vol. 527, p. 146790, Oct. 2020, doi: 10.1016/j.apsusc.2020.146790.

[48] Z. Han, J. Tian, Q. Lai, X. Yu, and G. Li, 'Effect of N2 partial pressure on the microstructure and mechanical properties of magnetron sputtered CrNx films', *Surf. Coat. Technol.*, vol. 162, no. 2, pp. 189–193, Jan. 2003, doi: 10.1016/S0257-8972(02)00667-9.

[49] T. B. Yaqub, T. Vuchkov, M. Evaristo, and A. Cavaleiro, 'DCMS Mo-Se-C solid lubricant coatings – Synthesis, structural, mechanical and tribological property investigation', *Surf. Coat. Technol.*, vol. 378, p. 124992, Nov. 2019, doi: 10.1016/j.surfcoat.2019.124992.

[50] J. C. Oliveira, F. Fernandes, F. Ferreira, and A. Cavaleiro, 'Tailoring the nanostructure of Ti–Si–N thin films by HiPIMS in deep oscillation magnetron sputtering (DOMS) mode', *Surf. Coat. Technol.*, vol. 264, pp. 140–149, Feb. 2015, doi: 10.1016/j.surfcoat.2014.12.065.

[51] W. Lauwerens *et al.*, 'Humidity resistant MoSx films prepared by pulsed magnetron sputtering', *Surf. Coat. Technol.*, vol. 131, no. 1, pp. 216–221, Sep. 2000, doi: 10.1016/S0257-8972(00)00796-9.

[52] J. Zhu, Q. Zeng, B. Zhang, C. Yan, and W. He, 'Elevated-temperature super-lubrication performance analysis of dispersion-strengthened WSN coatings: Experimental research and first-principles calculation', *Surf. Coat. Technol.*, vol. 406, p. 126651, Jan. 2021, doi: 10.1016/j.surfcoat.2020.126651.